Diurnal changes in the efficiency of information transmission at a sensory synapse

José Moya-Díaz, Ben James, Federico Esposti, Jamie Johnston and Leon Lagnado*

Sussex Neuroscience, School of Life Sciences, University of Sussex,
Brighton BN1 9QG, UK

*Corresponding author: l.lagnado@sussex.ac.uk

Abstract

Neuromodulators adapt sensory circuits to changes in the external world or the animal's internal state and synapses are key control sites for such plasticity. Less clear is how neuromodulation alters the amount of information transmitted through the circuit. We investigated this question in the context of the diurnal regulation of visual processing in the retina of zebrafish, focusing on ribbon synapses of bipolar cells. We demonstrate that contrast-sensitivity peaks in the afternoon accompanied by a four-fold increase in the average Shannon information transmitted from an active zone. This increase reflects higher synaptic gain, lower spontaneous "noise" and reduced variability of evoked responses. Simultaneously, an increase in the probability of multivesicular events with larger information content increases the efficiency of transmission (bits per vesicle) by factors of 1.5-2.7. This study demonstrates the multiplicity of mechanisms by which a neuromodulator can adjust the synaptic transfer of sensory information.

Introduction

It has long been understood that the flow of signals through neural circuits is adjusted by neuromodulators[1]. How does this plasticity translate into changes in the amount of information that is transmitted through the circuit? Here we investigate this question in the retina as visual processing adjusts on a diurnal cycle.

The retina is highly plastic: the input-output relation can adapt within seconds to the recent history of the visual stimulus[2,3] or, on longer time-scales, to changes in the animal's internal state[4,5]. In diurnal animals, for instance, retinal sensitivity to light is regulated both by the daily light-dark cycle and by intrinsic circadian clocks that act on both outer and inner retinal circuitry[6-9]. Key to these adjustments is dopamine, a neuromodulator which is released from amacrine cells in a circadian cycle, varying from a minimum at night, increasing during the day and peaking before dusk[6,10,11]. But the average luminance of a visual scene is not the variable driving most behaviours related to vision: navigation, finding food and avoiding predators all depend on detection of fast changes in light intensity. We therefore investigated the diurnal control of temporal contrast processing, focusing on the visual signal that bipolar cells transmit to the inner retina.

The synaptic compartments of bipolar cells represent an information bottleneck in vision because they are the only route for transmission of signals originating from photoreceptors. As a result, these compartments are an important control point for transformations of the visual signal[12] and contribute to a number of processing tasks, from adaptive gain control to temporal filtering and the coding of motion, colour, orientation and direction[3,13-15]. In common with other sensory neurons, such as photoreceptors, hair cells and electroreceptors, bipolar cells transmit information through ribbon synapses containing specialized structures that supply vesicles to the active zone[16]. These sensory synapses do not always operate as Poisson machines in which vesicles are released independently but also signal through multivesicular release (MVR), where the fusion of two or more vesicles is co-ordinated as a single synaptic

event[17-19]. The importance of MVR at a number of sites in the brain is now recognized and it has been suggested that it might contribute to more complex strategies for transmitting information than modulation of a rate code[20-22].

Shannon's information theory has been used to measure the amount of information carried by neurons using spikes, but these are not the neural events that transmit information across the synapse: there the essential symbol is the quantum of neurotransmitter released from a vesicle. To understand the information leaving a neuron the experimenter therefore needs to observe the fusion of vesicles conveying the message[23,24]. This has recently been achieved by multiphoton imaging of the glutamate reporter iGluSnFR[25] in the retina of larval zebrafish, where it is found that bipolar cells do not transmit the visual message using a simple binary code but instead use a number of symbols formed by one, two, three or more vesicles released as one event[19].

Here we demonstrate that the strategy of synaptic coding by amplitude as well as rate is under diurnal control. The Shannon information transmitted at each active zone increases four-fold in the afternoon compared to the morning and dopamine contributes to this increase by increasing synaptic gain, lowering spontaneous noise and reducing the variability of evoked responses. All three mechanisms operate in the OFF channel signalling decreases in light intensity, but only the last two in the ON channel signalling increases. Crucially, dopamine also adjusts the strategy by which these synapses code visual information by increasing the probability of multivesicular events with larger information content. Larger events carry more bits of information per vesicle so dopamine also increases the efficiency of the vesicle code.

Results

Differential regulation of luminance-sensitivity and contrast-sensitivity

To investigate the diurnal modulation of visual processing in the retina of zebrafish we began by imaging activity of the terminals of bipolar cells with a synaptically-localized calcium reporter, SyGCaMP2[26] (Fig. 1A). When animals were placed on a cycle of 14 hours light and 10 hours dark, no significant synaptic responses could be detected in the 6 hours preceding light onset (*Zeitgeber* times 18-0 hours), consistent with previous observations that larvae are blind at night[27]. Visual sensitivity began to recover within 20 mins of light onset, after which responses gradually increased in amplitude (Fig. S1A and Fig. 1B). Plotting the luminance-response functions (Fig. 1C) allowed the light sensitivity to be quantified as the inverse of the luminance generating a half-maximal response ($1/I_{1/2}$). Over the course of the day, luminance-sensitivity increased gradually over a range greater than 200-fold (Fig. 1D). As in other species, this increase could be explained largely by actions of D2 dopamine receptors because injection of the antagonist sulpiride (~2 μM) reduced luminance-sensitivity in the afternoon to levels measured in the morning[6] (Fig. S1).

The detection of modulations in light intensity was also under diurnal control, but with a different time-course (Fig. 1E-G; 5 Hz full-field stimuli). At ZT = 4 hours, temporal contrasts below 50% were barely detected and the half-maximal response ($C_{1/2}$) was generated by a contrast of 86 ± 2 % (Figs. 1E and F). But at ZT = 7 hours $C_{1/2}$ fell to 35 ± 2 % with responses saturated above 50% contrast. When contrast sensitivity ($1/C_{1/2}$) was mapped during the course of the day it was relatively constant at ZT 1-5 hours and ZT 9-14 hours but increased to levels ~2.4-fold higher around ZT = 7 hours (Fig. 1G). Notably, this peak in the contrast sensitivity of the retinal circuit occurred at a similar *Zeitgeber* time as the maximum contrast sensitivity measured behaviourally using the optokinetic reflex[9,28]. A qualitatively similar increase in contrast sensitivity was also observed at the retinal output projecting to the optic tectum (Fig. S2).

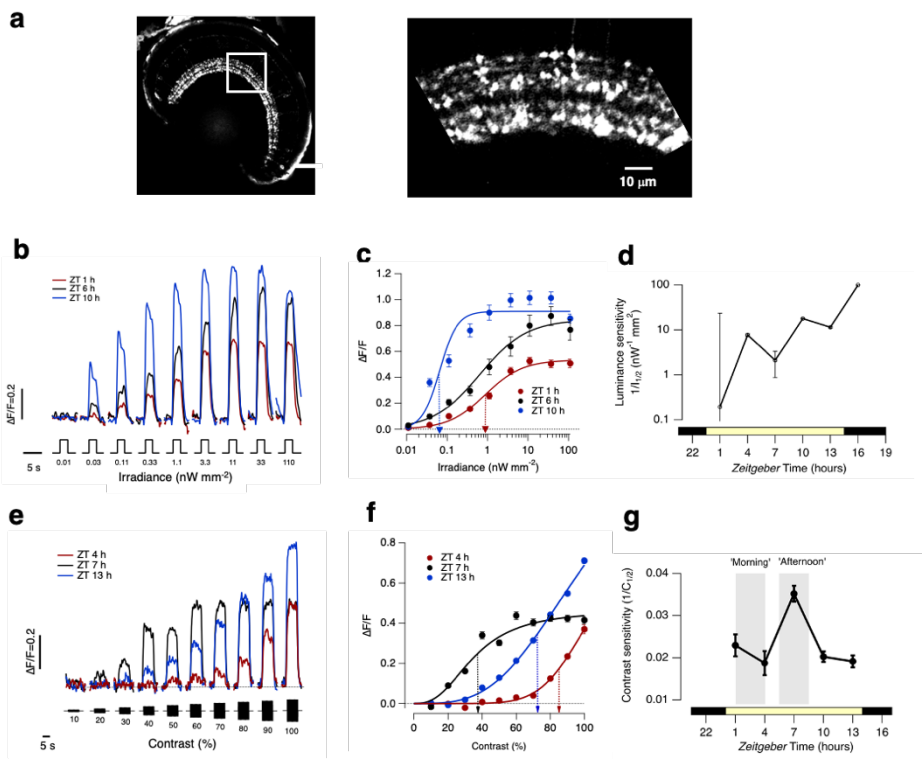

Figure 1: Differential regulation of luminance-sensitivity and contrast-sensitivity

A. Left: Retina of a Ribeye::SyGCaMP2 fish with box over the inner plexiform layer (IPL). Right: expansion of the boxed region showing terminals of bipolar cells. Zebrafish larvae were 7-9 days post-fertilization. **B.** Averaged responses from ON terminals to light steps of different irradiance measured at *Zeitgeber* time 1, 10 and 16 hours. Note large variations in amplitude and kinetics. The full-field light stimuli were generated by an amber LED (λ_{max} = 590 nm) which will most effectively stimulate red and green cones. Each light step lasted 3 s (*n* = 535 terminals from 10 fish). **C.** Peak response as a function of irradiance for ON terminals in B. The smooth lines are Hill functions of the form $R = R_{max}*(I^h/(I^h + I_{1/2}^h))$, where R is the peak response, I is the irradiance, h is the Hill coefficient and $I_{1/2}$ is the irradiance generating the half-maximal response. At ZT = 6 hrs: R_{max} = 0.91 ± 0.04; h = 2.0 ± 0.2; $I_{1/2}$ = 0.066 ± 0.02 nW/mm^2 (dashed blue arrow). At ZT = 10 hrs: R_{max} = 0.85 ± 0.06; h = 0.8 ± 0.1; $I_{1/2}$ = 0.65 ± 0.18 nW/mm^2. At ZT = 1 hrs: R_{max} = 0.853 ± 0.02; h = 0.9 ± 0.2; $I_{1/2}$ = 0.88 ± 0.18 nW/mm^2 (dashed red arrow). **D.** Variations in luminance sensitivity as a function of *Zeitgeber* time averaged across both ON and OFF terminals (n=535 and 335 terminals, respectively). The lower bar shows the timing of the light-dark cycle. Error bars are ± 1 SD. **E.** Averaged responses to stimuli of different contrasts (i.e. sinusoidal modulations in light intensity around a mean) measured at *Zeitgeber* time 4, 7 and 13 hrs averaged across both ON and OFF terminals (n = 949 from 21 fish). **F.** Peak response amplitude as a function of contrast for terminals shown in E. The smooth lines are Hill functions used to interpolate values of $C_{1/2}$, the contrast generating the half-maximal response. Note the diurnal variations. At ZT = 4 hrs: $C_{1/2}$ = 86 ± 2% (dashed red arrow); h = 7.0 ± 1.2. At ZT = 7 hrs: $C_{1/2}$ = 35 ± 2% (dashed black arrow); h = 2.7 ± 0.2. At ZT = 13 hrs: $C_{1/2}$ = 72 ± 2%; h = 3.3 ± 0.2 (dashed blue arrow). **G.** Variations in contrast-sensitivity as a function of *Zeitgeber* time averaged across ON and OFF terminals (n = 949 from 21 fish). Note the peak around ZT = 7 hours which is not mirrored in the diurnal variation in luminance sensitivity (D). The grey bars show the periods described as "morning" and "afternoon". All error bars show ± 1 SE except for D which is ± 1 SD.

135 **Diurnal regulation of contrast gain**

136 To explore the diurnal regulation of contrast sensitivity we measured transmission of the
137 visual signal to the inner retina in terms of its elementary units - synaptic vesicles - by
138 expressing the glutamate reporter iGluSnFR[25] sparsely in bipolar cells (Fig. 2A). A
139 variety of morphological types of bipolar cell were investigated but we focused on a
140 comparison of the two most basic functional groups, ON and OFF cells, identified
141 through their responses to steps of light (Fig. S3). Wiener deconvolution of iGluSnFR
142 signals allowed us to count released vesicles and evidence that these methods allow
143 the isolation of glutamatergic signals from individual active zones has been described[19]
144 (Fig. S4). Synaptic function was compared over a two-hour period centred on ZT = 1
145 hour ("morning") with a two-hour period centred on ZT = 7 hours ("afternoon"; Fig. 1G).

146 Examples of glutamate transients at the active zone of an OFF bipolar cell are
147 shown in Fig. 2B. Across a range of contrasts, responses were, on average, larger in
148 the afternoon. The contrast-response function (CRF) was constructed simply by
149 measuring the average number of vesicles released per cycle of a 5 Hz stimulus (full-
150 field), choosing this frequency because the integration time of a bipolar cell is ~200 ms[29].
151 There was little diurnal modulation of the CRF measured at ON synapses but in the OFF
152 channel the average synaptic gain, measured as the maximum rate of vesicle release
153 at 100% contrast, increased from 15.25 ± 2.5 vesicles/s in the morning to 25.5 ± 1.5
154 vesicles/s in the afternoon (Fig. 2C and D).

155

156

157

158

159

160

161

162

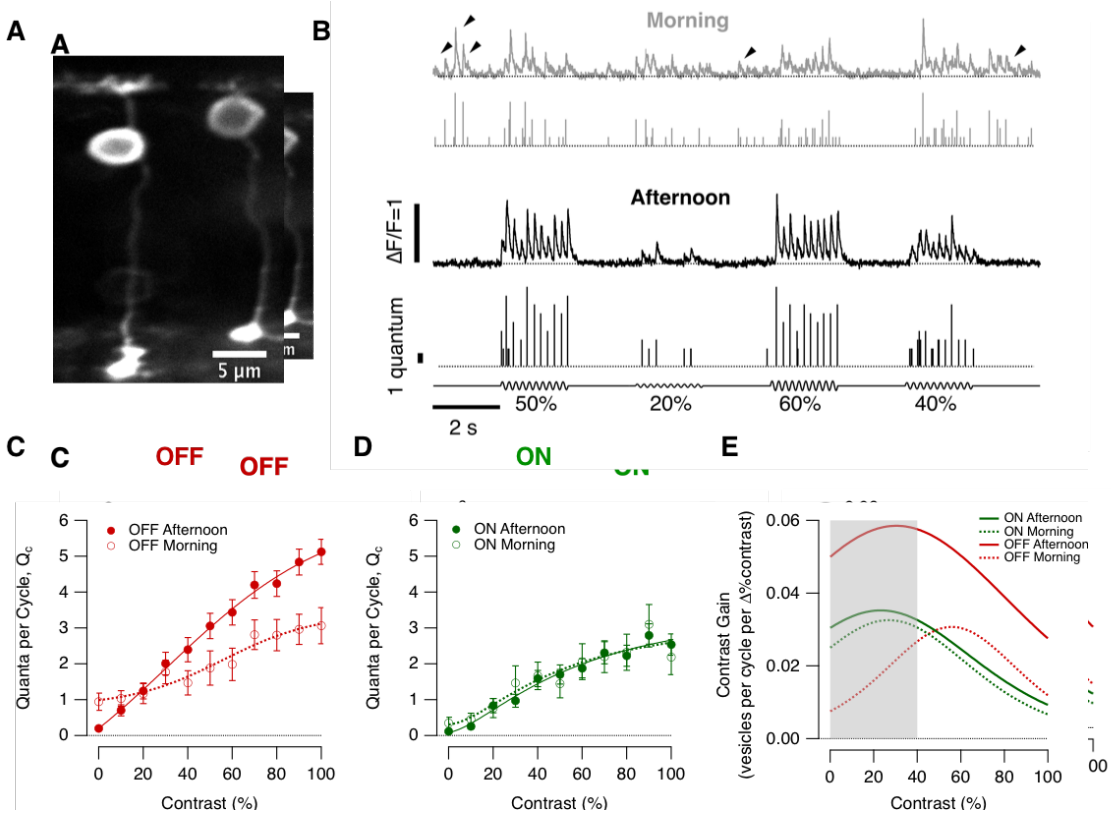

Figure 2. Diurnal modulation of synaptic gain

A. Multiphoton section through the eye of a zebrafish larva (7 dpf) expressing iGluSnFR in a subset of bipolar cells. **B**. Examples of iGluSnFR signals from an individual OFF synapse elicited using stimuli of variable contrast modulated at 5 Hz (0-100%, full field, sine wave) in the morning (ZT 0-2 hours, grey) and afternoon (ZT 6-8 hours, black). Note the high levels of spontaneous activity in the morning (black arrowheads). In each case the top trace shows the iGluSnFR signal and the lower trace the estimated number of quanta composing each event (Q_e). **C.** Average contrast-response functions in OFF bipolar cell synapses in the morning (open circles; n = 20 synapses) and afternoon (closed; n = 59), where the response (*R*) was quantified as the average of quanta per cycle, Q_c (i.e., the total number of quanta released *within* a single cycle of the sinusoidal stimulus). Each point shows the mean ± s.e.m The smooth lines are fits of a sigmoid used for smoothing. Note the differences in the shape of the contrast-response functions and in the levels of spontaneous activity (zero contrast) (One-way ANCOVA-test, $p<0.0006$). **D.** Average contrast-response functions in ON bipolar cell synapses in the morning (open circles; n = 12 synapses) and afternoon (closed; n = 31). There was no significant difference in the morning relative to afternoon. One-way ANCOVA-test, p = 0.53) Each point shows the mean ± s.e.m**. E.** The contrast gain calculated as the derivative of the fits to the contrast-response functions in C and D. The grey box provides an indication of the contrasts most common in nature (below about 40%). Note that the maximum contrast discrimination is increased by a factor of 2x in the OFF channel during the afternoon.

Increases in synaptic gain were accompanied by an increase in contrast sensitivity that shifted the CRF towards lower contrasts. To assess these combined effects we calculated the derivative of the CRF, which we term “contrast gain” (Fig. 2E). A second

reason for re-expressing the contrast response functions as "contrast gain" is that this gives insight into a key property of the visual system – it's ability to discriminate one stimulus from another[30,31]. Contrasts in natural visual scenes rarely exceed 40%[14] and in the morning changes in this range were signalled best through the ON channel (grey box in Fig. 2E). But in the afternoon the OFF channel became dominant, with contrast gains increasing by factors of 2-6 at contrasts up to 40%. Diurnal modulation of retinal processing therefore altered the relative importance of ON and OFF pathways in signalling temporal contrast.

Dopamine regulates contrast gain

Dopamine is a key regulator of the luminance-sensitivity of the retina[6,10,11]. To test whether this neuromodulator also adjusts contrast sensitivity we injected agonists or antagonists of dopamine receptors directly into the eye. Fig. 3A shows examples of the output from a synapse imaged in the afternoon, before and after injection of the D1 receptor antagonist SCH 23390 (estimated final concentration of 20 nM). Counteracting the actions of endogenous dopamine reduced the average rate of vesicle release and shifted the CRF such that the maximum contrast gain was achieved at higher contrasts (black points in Fig. 3B and C). Conversely, increasing activation of D1 receptors in the morning by injection of the agonist ADTN (~0.2 μM) increased response gain.

The dynamic range over which D1 receptors adjusted synaptic gain was calculated as the ratio of the CRFs in the presence of the agonist and antagonist ("relative response gain"): in both ON and OFF channels the maximum modulation was ~16-fold, occurring at contrasts of 20-40% (Fig. 3D). ~~But d~~Diurnal modulation of gain was narrower than this potential range, with a maximum of 1.7-fold in OFF synapses. This difference reflected, at least in part, a gain in the morning that was at least 5-fold higher than that measured with D1R receptors blocked, consistent with dopamine levels that were already high enough to potentiate synaptic transmission (Figs. 3B and C). These

manipulations of retinal dopamine receptors caused qualitatively similar changes in the signals that ganglion cells transmit to the optic tectum (Fig. S2).

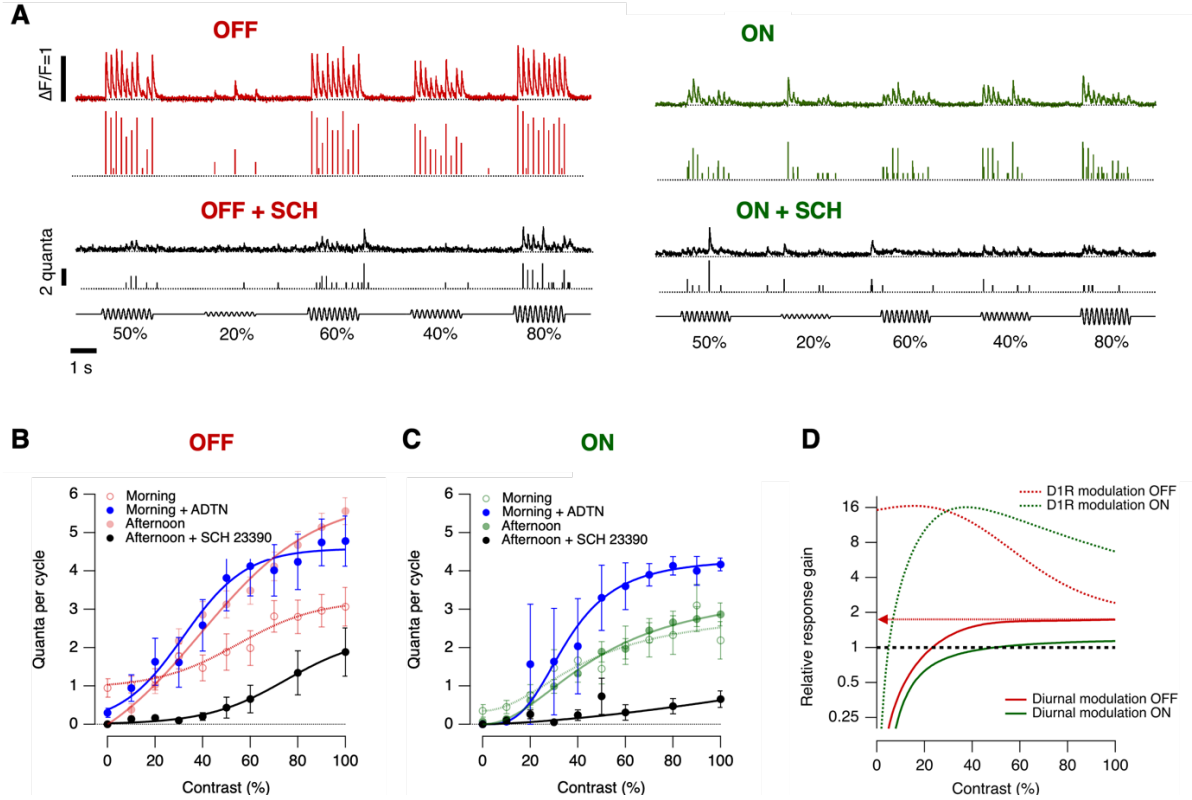

Figure 3. Diurnal changes in dopamine levels modulate synaptic transmission.

A. Examples of iGluSnFR signals recorded in the afternoon from an individual OFF (red trace) and ON (green trace) synapses elicited using a stimulus of variable contrast before and after intravitreal injection of the D1 antagonist, SCH 23390 (black traces; estimated final concentration 20 nM). Note that SCH 23390 abolished synaptic responses at lower contrasts in ON and OFF synapses. In each case the top trace shows the iGluSnFR signal and the lower trace the estimated Q_e. **B.** Average contrast-response functions in OFF bipolar cell synapses after administration of D1 antagonist (black dots) in the afternoon and after administration of the D1 agonist ADTN in the morning (blue dots). Each point shows the mean ± s.e.m. (SCH 23390, n =12 synapses; ADTN, n = 12 synapses). Control responses observed in the morning and afternoon are superimposed (red, from Fig. 2C). **C.** Average contrast-response functions in ON bipolar cell synapses after intravitreal injection of D1 antagonist in the afternoon (black dots) and ADTN in the morning (blue dots). Each point shows the mean ± s.e.m. (SCH 23390, n =7 synapses; ADTN, n = 5 synapses). Control responses observed in the morning and afternoon are superimposed (green, from Fig. 2D). **D.** Relative response gain by diurnal modulation and after manipulation of dopaminergic signalling (dashed lines). Note that diurnal modulation of synaptic gain is higher in OFF synapses, whereas dopamine modulates the dynamic range by ~16 fold-change in ON and OFF synapses.

268 **Modulation of synaptic noise and variability**

269 We next asked how diurnal changes in the operation of the retina affected the amount
270 of information that bipolar cells transmit to the inner retina. In the framework of
271 information theory[23], an increase in synaptic gain will tend to increase information about
272 a change in contrast by causing a larger change in the average number of vesicles
273 released. But the gain with which a synapse responds to a sensory signal is not the only
274 property that determines information transmission: neural information is degraded by
275 "noise" that causes responses to vary when the same stimulus is repeated and synapses
276 are a major source of such variability[32,33]. Synaptic noise is an inevitable consequence
277 of the stochasticity of the presynaptic processes that control the fusion of vesicles[20] and
278 such variability was a prominent feature of the output from synapses of bipolar cells, as
279 illustrated in Fig. 2B and Fig. 3A.

280 We distinguished four aspects of synaptic noise and investigated the diurnal
281 modulation of each; i) spontaneous vesicle release (Fig. 4), ii) variability in the number
282 of vesicles released by a stimulus (Fig. 5), iii) variability in the timing of release events
283 i.e how tightly they are time-locked to the stimulus (Fig. 6) and iv) changes in the
284 distribution of event amplitudes i.e modulation of multivesicular release (Fig. 7). Finally,
285 we calculated how these different aspects of synaptic noise combined with changes in
286 contrast gain (Fig. 3) to alter the amount of visual information transferred from individual
287 active zones (Fig. 8).

288

289

290

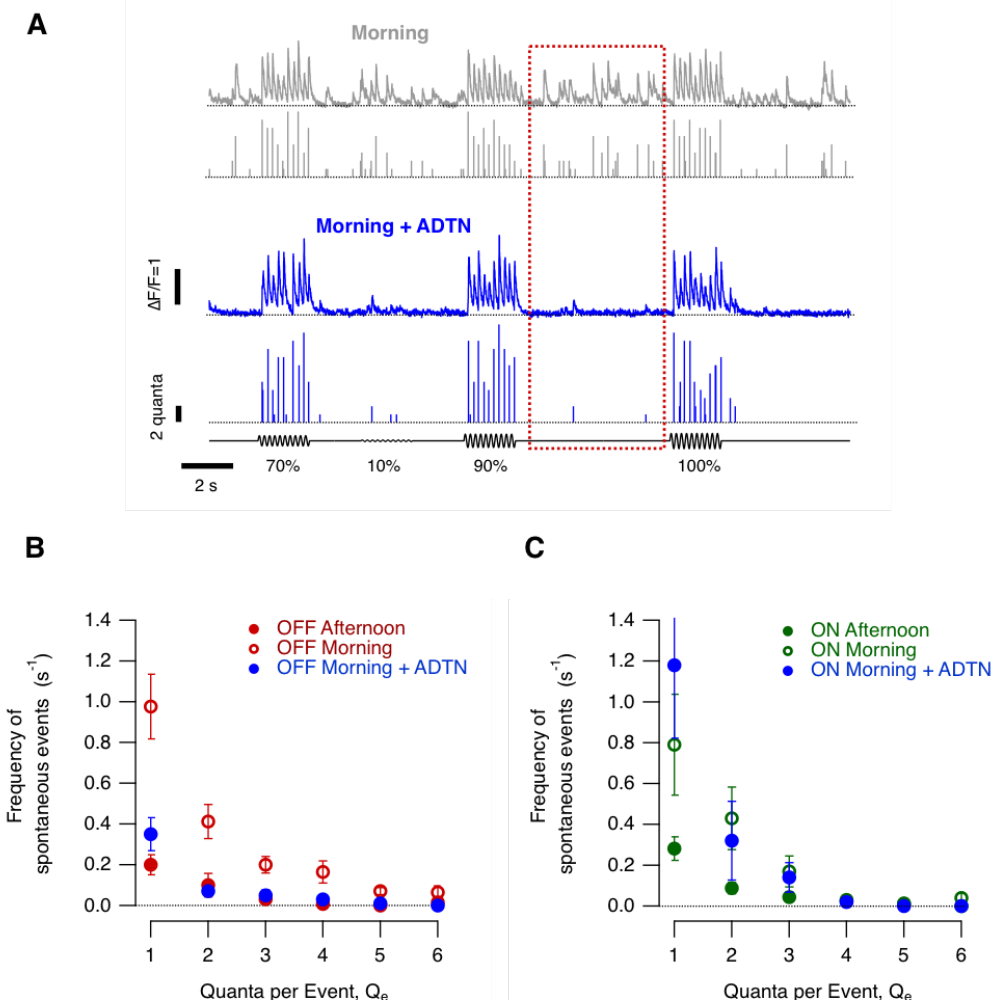

Figure 4. Diurnal modulation of spontaneous synaptic noise

A. *Top:* Example of iGluSnFR signals from an individual OFF synapse elicited using a stimulus of variable contrast in the morning (0-100%, 5 Hz modulation). In this example, note the high levels of spontaneous activity that were quantified as the responses elicited at zero contrast (red dashed box). *Bottom.* Examples of iGluSnFR signals from the same OFF synapse after intravitreal injection of ADTN. Note the increase in amplitude and frequency of events and the reduction of spontaneous activity. In each case the top trace shows the iGluSnFR signal and the lower trace the estimated Q_e. **B.** Quantification of spontaneous events composed by different Q_e in OFF synapses in the morning, morning + ADTN and afternoon (OFF morning, n = 20 synapses; OFF morning + ADTN n = 12 synapses; OFF afternoon, n = 24 synapses). Note the suppression of spontaneous events in OFF synapses after intravitreal injection of ADTN in the morning. Each point shows the mean ± s.e.m. **C.** Quantification of spontaneous events composed by different Q_e in ON synapses in the Morning, Morning + ADTN and Afternoon (ON Morning n = 12 synapses; ON Morning + ADTN n = 5 synapses; ON Afternoon, n = 17 synapses). Note that spontaneous activity levels were not dramatically altered after administration of ADTN. Each point shows the mean ± s.e.m.

308 ***i) Spontaneous release***

309 Increases in synaptic gain were accompanied by a *decrease* in the spontaneous release
310 of vesicles in the absence of a visual stimulus. In the morning, spontaneous events
311 occurred at relatively high rates, some composed of single vesicles and others of two or
312 more vesicles (Fig. 4A-C). Integrating across events of all amplitudes, the average rate
313 of spontaneous release in OFF synapses was 1.95 ± 0.04 vesicles s^{-1} in the morning,
314 falling to 0.37 ± 0.02 vesicles s^{-1} in the afternoon (Fig. 4B; significant at $p < 0.0001$, one-
315 way ANOVA). In ON synapses these values were 1.47 ± 0.09 vesicles s^{-1} and 0.46 ±
316 0.02 vesicles s^{-1} ($p < 0.0001$, Fig. 4C). Across both channels, therefore, spontaneous
317 noise was 3-5 times lower in the afternoon compared to the morning.

318 Spontaneous noise in OFF synapses was modulated by dopamine. Increased
319 activation of D1 receptors by injection of ADTN suppressed spontaneous release in the
320 morning to levels close to those measured in the afternoon (0.51 ± 0.03 vesicles s^{-1}), a
321 change significant at $p < 0.0001$ (one-way ANOVA; Fig. 4B). In contrast, ADTN had no
322 significant effect on spontaneous release from ON synapses (1.66 ± 0.18 vesicles s^{-1}, p
323 = 0.3; Fig. 4C).

324

325 ***ii) Variability in stimulus-evoked responses***

326 The reliability of neural responses measured as spikes can be expressed using the Fano
327 factor: the ratio of the variance-to-mean of spikes counted in a fixed time-window after a
328 repeated stimulus[34,35]. We used a similar approach to assess the reliability of synapses,
329 calculating the Fano factor (F) by counting the number of vesicles released over each cycle
330 of a sinusoidal stimulus (Fig. 5A). Through both ON and OFF channels, the variability of
331 synaptic output was significantly higher than expected for a Poisson process, for which the
332 Fano factor is one (Fig. 5B and C). This yields a fundamental insight: the ribbon synapses
333 of bipolar cells do not adhere to the common model of synaptic function in which all vesicles
334 are released independently.

335 In the morning, F was ~2.7 in both ON and OFF synapses when averaged over
336 contrasts of 10-100%, but synapses were more reliable in the afternoon, with F falling to
337 ~1.6 (One-Way ANOVA, $p<0.0001$; Fig. 5B-E). In the OFF channel, the increase in
338 contrast gain and sensitivity in the afternoon was therefore also associated with increased
339 reliability of bipolar cell synapses. Although synapses in the ON channel did not undergo
340 significant changes in gain and sensitivity, they also became more reliable. These diurnal
341 changes in synaptic reliability were also dopamine-dependent, activation of D1 receptors
342 in the morning reducing F to levels similar to those measured in the afternoon (Figs. 5D
343 and E).
344
345 ***iii) Temporal jitter***
346 Retinal ganglion cells (RGCs) encode information not just in their spike count but also in
347 the timing of spikes[34,36]. Spike times can vary by just a few milliseconds and this
348 accuracy depends on the precision of excitatory inputs received from bipolar cells[37]. The
349 standard deviation in timing of release events ("temporal jitter") was measured relative
350 to the phase of a 5 Hz stimulus (60% contrast; Fig. 6A) and the larger the release events
351 the more precise it was on average (Fig. 6B-C). In OFF synapses the temporal jitter was
352 5-8 ms higher in the morning compared to the afternoon for events composed of up to 8
353 vesicles (Fig. 6B; $p <0.008$, Kolomogorov-Smirnov test). Diurnal modulation of temporal
354 precision was weaker in ON synapses and only significant for events composed of 1-3
355 vesicles (Fig. 6C; t-test at each Q_e). Increasing activation of D1 receptors in the morning
356 reduced temporal jitter in events composed of multiple quanta in OFF synapses ($p <$
357 0.05; KS test) but not ON (Fig. 6B and C; $p > 0.5$). Diurnal variations in dopamine
358 therefore modulate the temporal accuracy of vesicle release in OFF synapses.

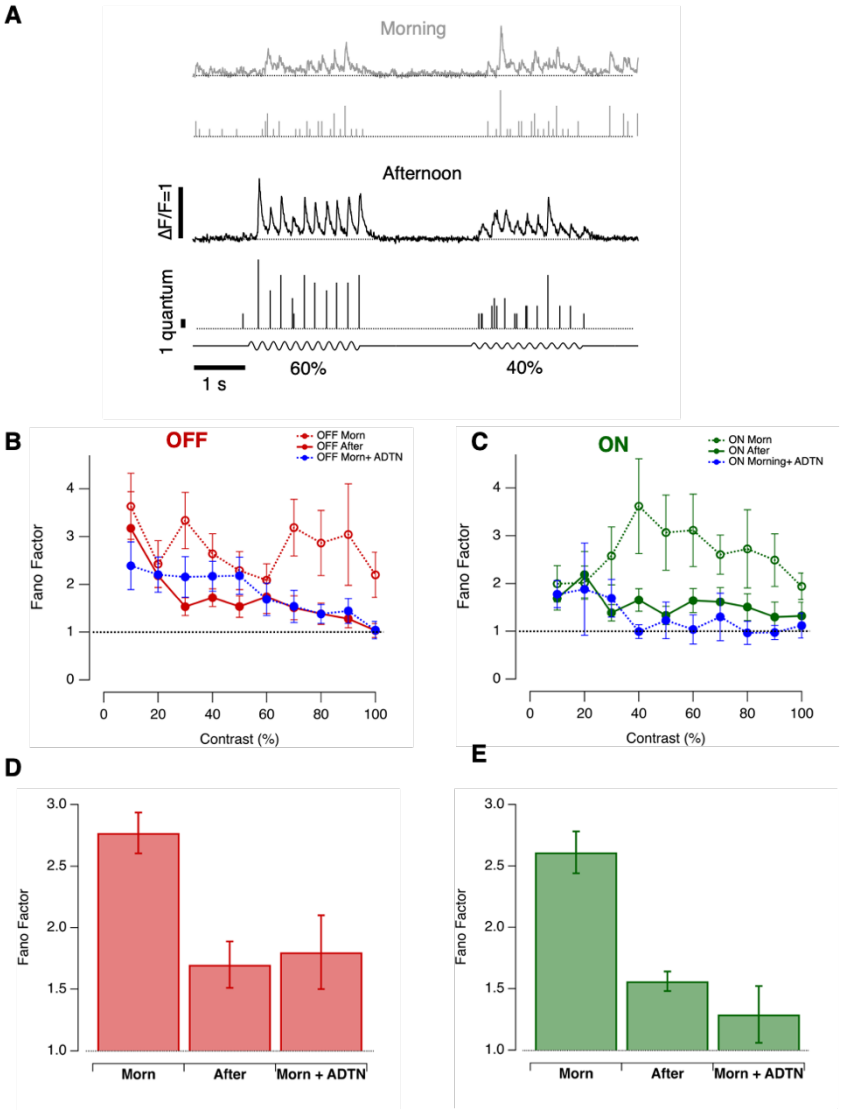

Figure 5. Diurnal changes in the variability of stimulus-evoked responses

A. Examples of iGluSnFR signals from individual OFF synapses in the morning and afternoon. Responses elicited by stimuli of 60% and 40% contrast varied from cycle to cycle of the 5 Hz stimulus. In each case the top trace shows the iGluSnFR signal and the lower trace the estimated Q_e. **B.** Variability in the response of OFF synapses calculated as the Fano factor, with each response measured as the total number of vesicles released over one cycle at each contrasts. Comparison is made between the morning (n = 18), afternoon (n = 27) and the morning after injection of ADTN (n = 13) Each point shows the mean ± s.e.m. **C**. As in B, but for ON synapses (n = 12, 15 and 6 synapses for respective conditions). **D.** Average Fano factor over different contrasts in OFF synapses in the three conditions described above. Data from B and C. Overall, the average Fano factor was significantly higher in the morning compared to afternoon or in the morning after injection of ADTN (One-Way ANOVA; $p<0.0001$). **E.** As D, but for ON synapses. Again, the average Fano factor was significantly higher in the morning (One-Way ANOVA; $p<0.0001$).

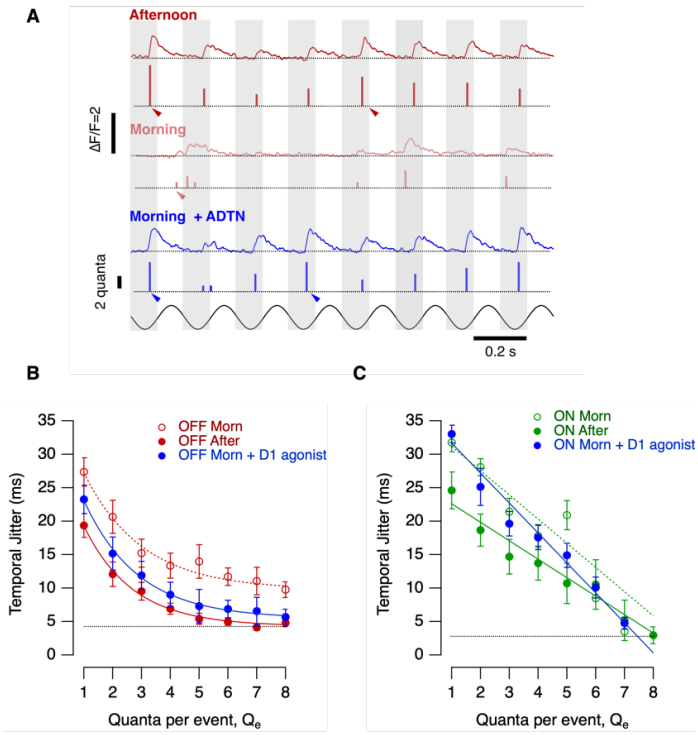

Figure 6. The temporal precision of vesicle release is under diurnal control in the OFF channel

A. Example recordings from two OFF synapses stimulated at 60% contrast in three conditions: afternoon (top, black trace), morning (middle, red trace) and after intravitreal injection of ADTN in the morning (bottom, blue trace). Morning and morning + ADTN synaptic responses are from the same synapse. The modulation in intensity (5 Hz, sine wave) is shown below. Arrowheads highlight events occurring at different phases of the stimulus, with less variation with events composed for 4 or more quanta in the afternoon and after administration of ADTN in the morning. In each case the top trace shows the iGluSnFR signal and the lower trace the estimated Q_e. **B.** Temporal jitter of events composed of different numbers of quanta in OFF synapses in the afternoon (red dots ; n = 24 synapses); Morning (open red dots; n = 19 synapses) and Morning + ADTN (blue dots, n = 16). Note that during the morning events composed by multiple quanta were less phase-locked to the stimuli in comparison to the afternoon. Activation of D1 receptors had a significant effect on release of multiquantal events. Events composed by 5 or more quanta jittered by ~5 ms, similar to values observed in the afternoon (black dashed line). The solid lines describing these relations in the three conditions are better described by a single exponential decay function of the form $y_0 + A_{exp}((-(x-x_0)/\tau)))$ with y0= 4.23 ± 1.2 and A = 27 ± 7 in the afternoon; y0= 9.77 ± 1.4 and A= 28.64 ± 5.6 in the morning and y0=5.45 ± 1.3, A = 30. ± 6.1 after activation of D1 receptor in the morning. **C.** Temporal jitter of events composed by different numbers of quanta measured in ON synapses in the afternoon (green dots; n = 14 synapses) during the morning (open green dots; n= 10 synapses) and during Morning + ADTN, (blue dots; n=6 =synapses). Activation of D1 receptor did not have a significant effect in the temporal precision in the ON channel. The relationships observed in the different conditions were better described by a straight line. Morning a = 34.7 ± 1.5 and a slope = -3.6 ± 0.5; Afternoon: a = 25.1 ± 1.2 and a slope = -2.8 ± 0.2; Morning + ADTN a = 34.9 ± 1.5 and a slope = -4.2 ± 0.3. Note that events composed of 8 or more quanta jittered by just ~ 4 ms (black dashed line).

397 ***iv) Changes in the distribution of multivesicular events***

398 Previous studies quantifying the synaptic transfer of visual information have been limited
399 by the inability to monitor individual active zones and used the assumption that vesicles
400 are released according to Poisson statistics[38,39]. But we now know that bipolar cells do
401 not employ a simple rate-code and visual information is also contained in the *amplitude*
402 of multivesicular events[19]. We therefore tested whether modulation of contrast gain was
403 accompanied by changes in the way stimulus contrast was encoded by the distribution
404 of Q_e, the number of quanta in an event, and found that it was.

405 A comparison of the distribution of Q_e in the morning and afternoon is shown in Fig.
406 7 for responses to a stimulus of 60% contrast. In ON synapses, 68% of release events
407 in the morning were univesicular, falling to 40% in the afternoon as the distribution
408 shifted towards larger MVR events (Fig. 7B; $p < 0.05$, KS test). This shift was fully
409 reversed by antagonizing D1 receptors by injection of SCH 23390 (Fig. 7C; $p < 0.001$).
410 In the morning, MVR was more prevalent in OFF synapses than ON, with only 38% of
411 release events being univesicular but again there was a significant shift towards larger
412 events in the afternoon (Fig. 7D; $p<0.02$). Blocking the D1 actions of endogenous
413 dopamine had a stronger effect in OFF synapses, increasing the proportion of
414 univesicular events to 66% in the afternoon (Fig. 7E; $p < 0.001$). Qualitatively similar
415 modulation of MVR was observed over a range of contrasts from 20% to 80% and
416 blocking D1 receptors in the afternoon shifted the distribution back to univesicular
417 release in both ON and OFF channels.
418
419
420
421
422
423

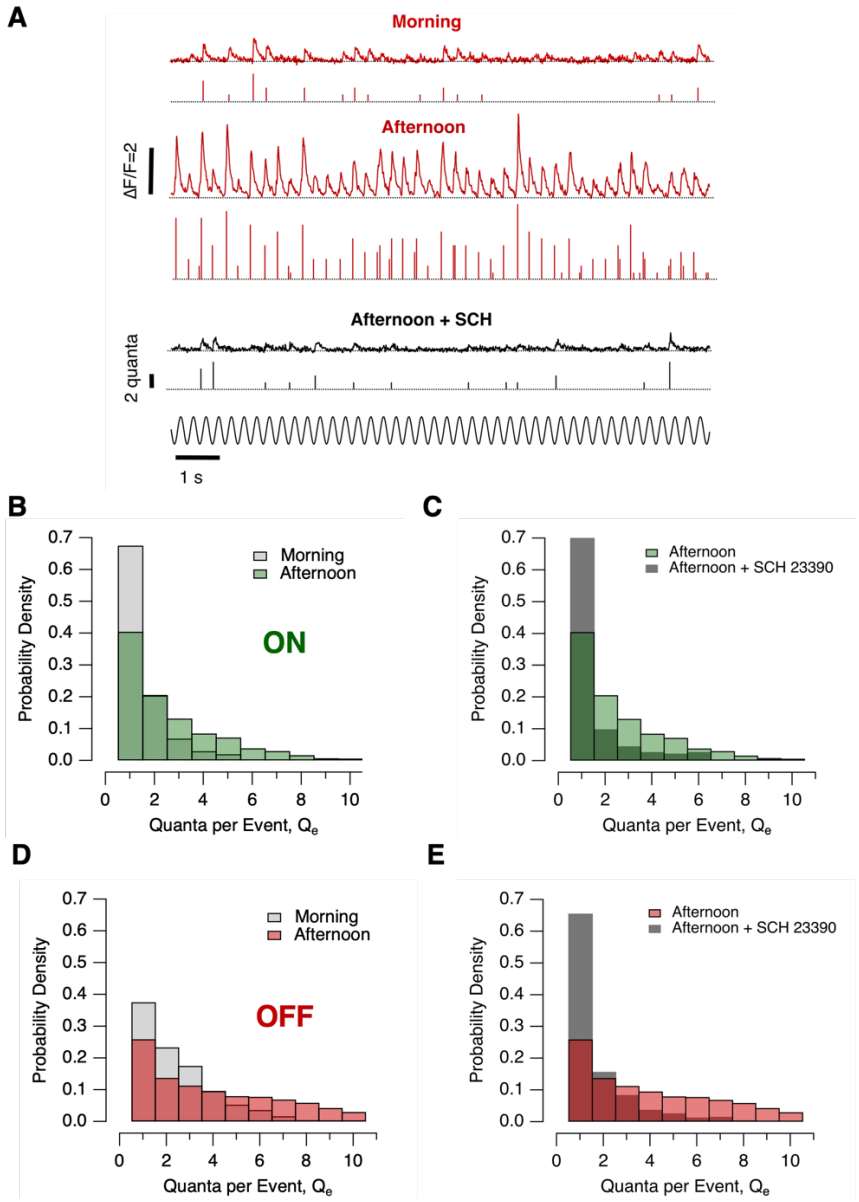

Figure 7. Dopamine contributes to diurnal variations in the distribution of multivesicular events

A. Examples of iGluSnFR signals from individual OFF synapses elicited using 60% contrast stimulus (5 Hz, 30 sec) in the morning (top), afternoon (middle) and afternoon + SCH 23390 (bottom). In each case the top trace shows the iGluSnFR signal and the lower trace the estimated Q_e. **B**. Changes in Q_e in ON synapses in the morning (light grey bars, n = 10 synapses) and afternoon (green bars, n = 14 synapses). In the afternoon the distribution was shifted toward multiquantal events ($p<0.05$, KS-test). **C.** Changes in the distribution of Q_e in ON synapses before and after intravitreal injection of the D1 antagonist SCH23390 (dark grey bars, n = 8 synapses). The distribution was shifted toward lower Q_e ($p<0.001$) but was not significantly different to that measured in the morning. **D.** Changes in Q_e, in OFF synapses in the morning (light grey bars, n = 19 synapses) and afternoon (red bars, n = 24 synapses). In the afternoon the distribution was shifted toward multiquantal events ($p<0.02$). **E.** Changes in the distribution of Q_e in OFF synapses before and after intravitreal injection of SCH 23390 in the afternoon (dark grey bars, n = 12 synapses). The distribution was shifted toward uniquantal events ($p<0.001$).

439 **Modulation of information encoded at the synapse**

440 How do changes in synaptic gain (Figs. 2-3), variability (Fig. 4-6) and MVR (Fig. 7)
441 combine to alter the amount of visual information transmitted by the synapses of bipolar
442 cells? A larger signal relative to noise will tend to increase the mutual information (I)
443 between the response (Q) and the stimulus generating it (S), although the size of the
444 increase will depend on the statistical properties of both signal and noise[40]. But how
445 should we quantify the synaptic signal? When analyzing the spike code, all events
446 comprise the same symbol and the response can be described as the number of spikes
447 in each of a series of time bins[24,40]. The output from bipolar cells is qualitatively different
448 with a visual stimulus being encoded both by the timing of release events and their
449 amplitudes[19]. We therefore took an approach in which MVR events composed of
450 different numbers of vesicles were considered different symbols for the conveying of
451 information[23,41]. The mutual information between the response and stimulus was then
452 computed as the average amount of information about the stimulus gained from
453 observing any symbol (see Methods).

454 The stimulus set S comprised 11 different contrasts but these were not fixed for each
455 synapse because the contrast sensitivity varied between synapses and between
456 morning and afternoon (Fig. 1E-G). To make allowance for this, we used contrasts
457 spanning ±10% around $C_{1/2}$ measured within the synapse under study immediately
458 before delivering the stimulus set. In the absence of information about the distribution of
459 contrasts normally experienced by a larval zebrafish, a uniform distribution of contrasts
460 was used for S. Each contrast step lasted 2 s (5 Hz) and they were presented in two
461 different pseudo-random orders, of which one is shown in Fig. 8A.

462 In the morning, the average mutual information between stimulus and response was
463 almost exactly the same for synapses in the ON and OFF channels (0.45 ± 0.04 bits s^{-1}
464 and 0.46 ± 0.03 bits s^{-1}, respectively). In the afternoon mutual information increased
465 through both channels although the increase in OFF synapses (370%) was significantly
466 larger than in ON (270%; KS test, $p < 0.001$; Fig. 8B). In OFF synapses, the maximum

467 mutual information of 2.1 bits s^{-1} was associated with an average release rate of 2.5

468 vesicles s^{-1} around $C_{1/2}$ (Fig. 2C), equivalent to an efficiency of ~0.8 bits per vesicle.

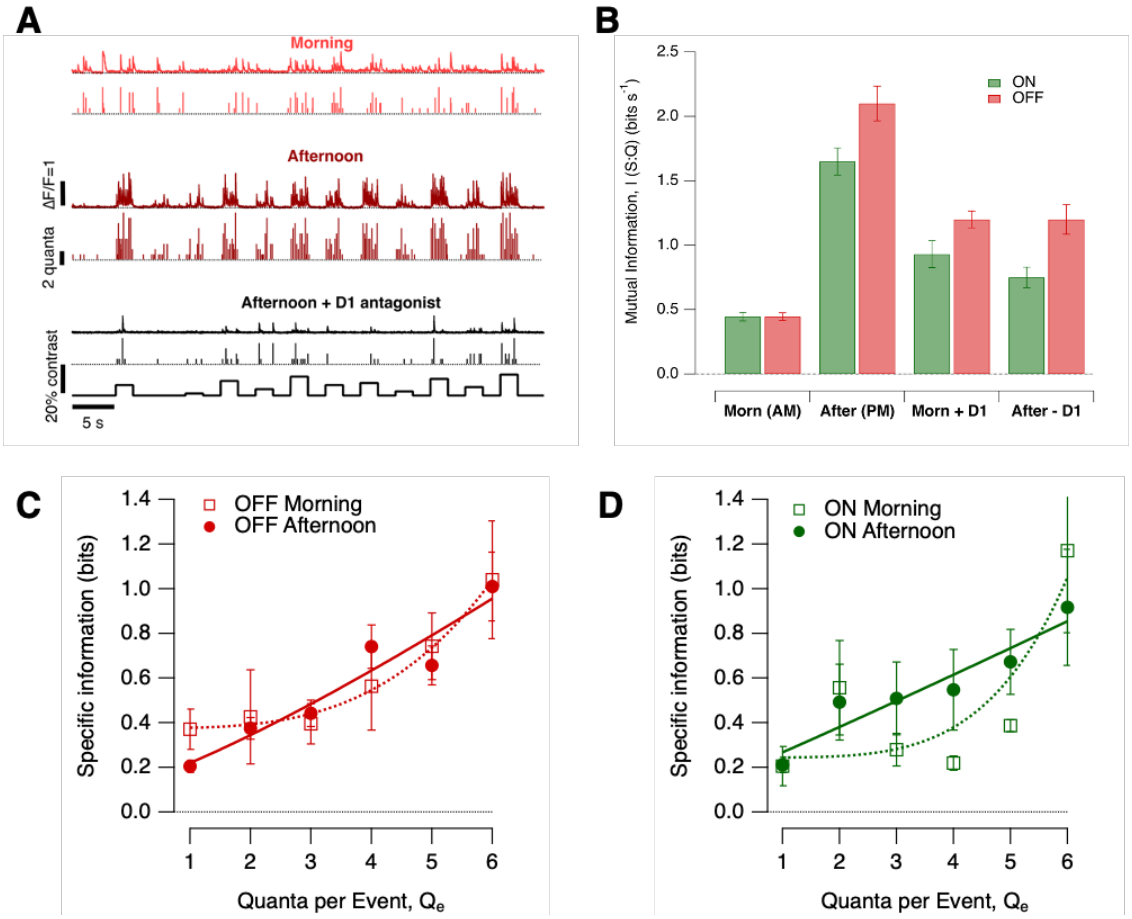

469

470 **Figure 8. Diurnal changes in the efficiency with which synapses transmit visual information**

471 **A.** Examples of synaptic responses over 11 different contrasts spanning ±10% around the contrast
472 eliciting the half-maximal response ($C_{1/2}$) in the morning (top, light red), afternoon (middle, dark red) and
473 after injection of D1 antagonist SCH 23390 in the afternoon (bottom, black; note the lower frequency and
474 amplitude of release events). In each case the top trace shows the iGluSnFR signal and the lower trace
475 the estimated Q_e. Each contrast step lasted 2 s (5 Hz) and each trace is from a different OFF synapse. **B.**
476 Mutual information *I (S:Q)* in four conditions: morning (Morn AM; OFF = 15 synapses, ON = 10 synapses),
477 afternoon (After PM; OFF = 33 synapses , ON= 13 synapses), morning after injection of ADTN (Morn + D1;
478 OFF = 14 synapses, ON = 6 synapses) and afternoon after injection of SCH 23390 (After - D1; OFF= 12
479 synapses, ON = 6 synapses). Differences between morning and afternoon were significant at $p<0.0001$
480 (One-way ANOVA), as were the effects of drug manipulations. **C.** Specific information (*I*) for events of
481 different quantal content in OFF synapses (morning, n = 15; afternoon, n = 33). The curve describing the
482 relation are least-squares fit of a power function of the form $I = y0 + AQ_e^x$. In the morning, y0 = 0.38, A =
483 0.0017, x = 3.4. In the afternoon, y0 = 0.12, A = 0.10, x = 1.2. **D.** As C, but for ON synapses (morning, n =
484 10; afternoon, n = 13). In the morning, y0 = 0.24, A = 0.0003, x = 4.4. In the afternoon, y0 = 0.16, A = 0.11,
485 x = 1.0.

486 Several of the synaptic properties we have analyzed will contribute to the
487 improvement in information transmission in the afternoon, including the increase in
488 synaptic gain (Fig. 2), the decrease in spontaneous noise (Fig. 3) and reduced variability
489 of stimulus-evoked responses (Figs. 5 and 6). All these aspects of synaptic transmission
490 were subject to modulation by dopamine and, consistent with these changes, the mutual
491 information in the morning was increased by activation of D1 receptors while in the
492 afternoon it was decreased by antagonizing the effects of endogenous dopamine (Fig.
493 8B). Antagonizing D1 receptors did not, however, reduce mutual information to levels
494 measured in the morning, leaving open the possibility that other signaling pathways or
495 other neuromodulators also contribute to diurnal changes in the signaling of temporal
496 contrast.
497
498 **Changes in the efficiency of the vesicle code**
499 The transfer of information through neural circuits using spikes and vesicles is the major
500 consumer of energy in the brain with one estimate being of the order of ~24,000 ATP
501 molecules per bit[42,43]. The largest part of this energy consumption is taken up by
502 synaptic transmission so a key question becomes the effect of neuromodulation on the
503 efficiency with which vesicles are used. Strikingly, the 2.7-fold increase in information
504 transmitted through ON synapses in the afternoon (Fig. 8B) was *not* associated with any
505 change in the average rate of vesicle release (Fig. 2D and E), while the 3.7-fold increase
506 in OFF synapses was associated with only a 2-fold increase in the rate around $C_{1/2}$ (Fig.
507 2C and E). The diurnal increase in synaptic gain was therefore associated with a 1.4-
508 to 2.7-fold increase in the average efficiency with which vesicles were used to encode
509 changes in contrast.
510 How is this increase in the efficiency of the vesicle code achieved? The simple
511 comparison of information transmission with average rates of vesicle release obscures
512 the fact that information about contrast is represented as changes in both the rate and
513 amplitude of release events[19]. This hybrid coding strategy is significant because the

514 distribution of MVR events is also a function of *Zeitgeber* time and larger events are rarer
515 and carry more specific information, as shown in Fig. 8C and D. Averaging across ON
516 and OFF channels and times of day, univesicular events carried 0.25 ± 0.03 bits of
517 information while events comprising 6 vesicles contained 1.03 ± 0.14 bits (equivalent to
518 0.17 bits per vesicle). Diurnal changes in the efficiency of the vesicle code therefore
519 depend on the electrical and biochemical processes that determine the fusion of vesicles
520 in the synaptic compartment.
521
522
523 **Discussion**
524 The plasticity of synapses allows the flow of information through circuits to be
525 modulated[1] and this study provides a quantitative understanding of this idea in the
526 context of the diurnal control of visual processing in the retina. The physiology of this
527 circuit is regulated by circadian clocks intrinsic to photoreceptors and neurons in the
528 inner retina and these become entrained by light and dopamine[7,45-47]. We find that this
529 cycle alters the transmission of visual information through bipolar cells by factors of ~4
530 during daylight hours by adjusting four synaptic properties; the number of vesicles
531 released by a stimulus (Fig. 3), spontaneous synaptic noise (Fig. 4), the variability of
532 stimulus-driven responses (Figs. 5-6) and the balance between univesicular and
533 multivesicular release (Fig. 7). Crucially, the shift towards MVR events of larger
534 amplitude also increases the amount of information transmitted per vesicle (Fig. 8).
535 Dopamine plays a major role in regulating all these aspects of retinal function although
536 the relative contributions of these mechanisms differed between ON and OFF pathways.
537 In the ON pathway, for instance, the reduced variability of synaptic responses and
538 increased emphasis on MVR increased information transfer *without* an increase in
539 synaptic gain or decrease in spontaneous noise.
540

541 **Diurnal modulation of gain**

542 Dopamine-dependent changes in the synaptic gain of bipolar cells might be caused
543 either by direct modulation of processes within the terminal compartment and/or by
544 actions on the circuitry in which they are embedded. Evidence for direct actions is
545 provided by electrophysiological experiments in bipolar cells isolated from the retina of
546 goldfish which show that activation of D1Rs potentiate the L-type calcium channels that
547 control vesicle release[4]. We now need to improve our understanding of which types of
548 bipolar cell might are under the strongest modulatory control. In mice, D1Rs are found
549 on the terminal compartment of bipolar cells driven by cones[48,49] but in zebrafish we only
550 know that D1 receptors identified by *in situ* hybridization are found in most cell types of
551 retina[50]. We also need to understand whether calcium channels are the only target of
552 dopamine acting directly on bipolar cell terminals because capacitance measurements
553 also demonstrate diurnal modulation of processes downstream of the calcium signal:
554 the efficiency with which calcium triggers vesicle release is higher during the day
555 compared to night, reflecting higher numbers of synaptic ribbons attached to an active
556 zone[51].

557 Beyond the terminal itself, dopamine receptors of different types are found on most
558 major classes of retinal neuron, where they can modulate both chemical and electrical
559 synapses to adjust the luminance sensitivity of the retinal circuit[8]. Less clear is how
560 dopamine acting at these other targets might be involved in diurnal control of contrast
561 sensitivity. Activation of D2 receptors on cone synapses can potentiate the visual drive
562 to bipolar cells but this mechanism alone does not easily explain the *transient* increase
563 in contrast-sensitivity in the afternoon given that luminance sensitivity, a much more
564 direct reflection of the strength of cone output, gradually increases throughout the day
565 (cf. Fig. 1B and Fig. 1E). The output from bipolar cells is also strongly dependent on the
566 inhibitory signals that the synaptic compartments receive from amacrine cells. In mice,
567 the activation of D1 receptors reduces inhibitory inputs that OFF cone bipolar cells
568 receive from narrow-field glycinergic amacrine cells[52], while D1 receptors on a subset of

569 wide-field GABAergic amacrine cells reduce inhibitory inputs onto the terminals of rod
570 bipolar cells[53]. The possibility of diurnal modulation of inhibition remains open
571 There is a good possibility that neuromodulators other than dopamine will also act
572 on the synaptic output of bipolar cells, either directly or indirectly, to regulate the visual
573 signal transmitted to ganglion cells. Amacrine cells release a number of neuroactive
574 substnces, including melatonin[54], Substance P[55] and somatostatin[56] and some of these
575 can antagonize the actions of others[55]. A large number of different proteins control the
576 activity of the retinal circuit and 17% of genes in zebrafish are under circadian
577 regulation[7].
578
579 **Diurnal modulation of variability**
580 It has long been appreciated that synaptic noise can reduce the amount of information
581 transmitted through a circuit of neurons[32]. When the retina operates under photopic
582 conditions, for instance, the release of vesicles from bipolar cells adds noise to the signal
583 arriving from cones and therefore causes a loss of information in RGCs[57]. It has been
584 suggested that under other circumstances the noise in synaptic transmission might
585 *improve* information transmission, such as when stochastic resonance increases the
586 probability of post-synaptic depolarization crossing threshold for spike generation[33,58]. It
587 seems unlikely, however, that the retina of zebrafish operates under such a regime,
588 given that diurnal increases in synaptic gain went hand-in-hand with a *reduction* in
589 several sources of noise, including spontaneous release unrelated to a stimulus.
590 The variability in the synaptic response of bipolar cells were quantified as average
591 Fano factors of 1.7-2.6 (Fig. 5B-E) but the spike responses of post-synaptic ganglion
592 cells have been reported to be more reliable, occurring with Fano factors varying from
593 1.5 at low contrasts down to 0.3 at higher contrasts[34]. The lower variability of responses
594 in RGCs is not unexpected given that these neurons integrate signals from multiple
595 bipolar cell synapses, but we now need to understand how far noise at this stage of the

596 visual system is also diurnal control. Ultimately, the variability of signals leaving the
597 retina should be compared with the variability of the behavioural responses they drive.
598 The variability of neural responses is a key determinant of the amount of information
599 they can carry. Vesicles released individually contained 0.25 bits of information (Fig. 8C
600 and D). A comparison can be made with the information transmitted by spikes in RGCs,
601 where the most sluggish cells transmit ~3.5 bits/spike, while those that fire most briskly
602 encode ~2 bits/spike[44]. A spike in an RGC therefore contains about ten times as much
603 information about a visual stimulus as a glutamatergic vesicle released from a bipolar
604 cell. This ratio is likely to vary between different functional types of RGC. It is notable
605 that an increase in spike rate is associated with a *decrease* in the amount of information
606 per spike[44] while an increase in vesicle release rate is associated with an *increase* in
607 information per vesicle.
608 All the aspects of synaptic function that we compared in the morning and afternoon
609 were sensitive to the activation of D1 receptors, indicating that dopamine adjusts
610 information transmission by orchestrating changes in both the signal and the various
611 noise sources that cause it to vary. The balance between modulation of signal and noise
612 was, however, strikingly different in the ON channel, where synaptic gain was *not* under
613 diurnal modulation, compared to the OFF channel, where both signal and noise were
614 regulated. Why? The significance of this differential modulation of ON and OFF channels
615 is unclear, but it may be related to the distributions of positive and negative contrasts in
616 the watery environment. Regardless of our ability to answer the "Why?" question, we
617 need to understand the processes by which dopamine and other neuromodulators adjust
618 synaptic noise. These are likely to involve both direct actions on the synaptic
619 compartment and indirect actions on other components of the retinal circuit. For
620 instance, inhibitory inputs from amacrine cells inject noise into the terminal of bipolar
621 cells[59] and it may be that dopamine receptors on amacrine cells modulate this source of
622 variability.
623

624 **Modulation of multivesicular release**

625 MVR is not just a property of ribbon synapses but is also a feature of synaptic
626 transmission in the hippocampus[60], cerebellum[61] and somatosensory cortex[21], where
627 arrival of a spike can often trigger release of two or more vesicles at an active zone. A
628 recent combination of electrophysiology with correlative light-and electron-microscopy
629 has even led to the suggestion that MVR may be a fundamental mode of synaptic
630 transmission throughout the nervous system[22]. It is also recognized that MVR can be
631 adjusted by neuromodulation, for instance through muscarinic acetylcholine receptors
632 in the striatum[62] or $GABA_B$ receptors in the cortex[63], although the implications for
633 information transmission in these contexts is not known. Our study has demonstrated
634 that potentiation of MVR in the retina not only increases the amount of information that
635 a synapse can transmit but also the efficiency of the vesicle code. It will be interesting
636 to establish how far neuromodulators acting in other parts of the brain alter the efficiency
637 of the information transmission and whether this involves modulation of gain as
638 compared to the noise that is a prominent feature of many central synapses[32,33].

639 In the future we will need to understand not just how the information carried by
640 vesicles is modulated, but also how this impacts on the information contained in the
641 spikes generated postsynaptically. How do changes in the vesicle code affect the spike
642 code?

643
644

645

646 # Methods

647

648 **Zebrafish husbandry**

649 Fish were raised and maintained under standard conditions on a 14 h light/10 h dark
650 cycle[39]. To aid imaging, fish were heterozygous or homozygous for the casper mutation
651 which results in hypopigmentation and they were additionally treated with1-phenyl-2-
652 thiourea (200 μM final concentration; Sigma) from 10 hours post fertilization (hpf) to reduce
653 pigmentation. All animal procedures were performed in accordance with the Animal Act
654 1986 and the UK Home Office guidelines and with the approval of the University of Sussex
655 Animal Welfare and Ethical Review Board. More information about experimental design
656 and reagents is available in the Life Sciences reporting Summary. The composition of the
657 E2 medium in which experiments were carried out was as follows: Na_2HPO_4 0.05 mM,
658 $MgSO_4$ 1mM, KH_2PO_4 0.15 mM, KCl 0.5 mM, NaCl 15 mM. CaCl 1mM, $NaHCO_3$ 0.7 mM,
659 pH 7.0-7.5.

660

661 **Transgenic fish**

662 Experiments were carried out using the following transgenic lines of zebrafish:

663 i) *Tg(ribeye:Zf-SyGCaMP2)* expressing the synaptically-localized fluorescent calcium
664 reporter SyGCaMP 2.0 in retinal bipolar cells under the ribeye-A promoter[26].

665 *ii) Tg(–1.8ctbp2:Gal4VP16_BH)* fish that drive the expression of the transcriptional
666 activator protein Gal4VP16 were generated by co-injection of I-SceI meganuclease and
667 endofree purified plasmid into wild-type zebrafish with a mixed genetic background. A
668 myocardium-specific promoter that drives the expression of mCherry protein was
669 additionally cloned into the plasmid to allow for phenotypical screening of founder fish.

670 *iii) Tg(10xUAS:iGluSnFR_MH)* fish driving the expression of the glutamate sensor
671 iGluSnFR under the regulatory control of the 10 x UAS enhancer elements were generated
672 by co-injection of purified plasmid and tol2 transposase RNA into offspring of AB wildtype

673 fish outcrossed to casper wildtype fish. The sequences for the myocardium-specific
674 promoter driving the expression of enhanced green fluorescent protein (mossy heart) were
675 added to the plasmid to facilitate the screening process.
676 iv) *Tg(–1.8ctbp2:SyGCaMP6)* fish were generated by co-injection of I-SceI
677 meganuclease and endofree purified plasmid into wild-type zebrafish with a mixed genetic
678 background. The GCaMP6f variant was kindly provided by L. Looger (Janelia Farm). This
679 variant holds a T383S mutation in comparison to the commercially available GCaMP6-fast
680 version (Addgene plasmid 40755).
681 v) *Tg(isl2b:nlsTrpR, tUAS:memGCaMP6f)* which drives the expression of memGCaMP6f
682 in the optic tectum was generated by co-injecting pTol2-isl2b-hlsTrpR-pA and pBH-tUAS-
683 memGaMP6f-pA plasmids into single-cell stage eggs. Injected fish were out-crossed with
684 wild-type fish to screen for founders.
685
686 **Multiphoton Imaging *In Vivo***
687 Experiments were carried out in a total of 117 zebrafish larvae (7–9 days post-fertilization).
688 Fish were immobilized in 3% low melting point agarose (Biogene) in E2 medium on a glass
689 coverslip (0 thickness) and mounted in a chamber where they were superfused with E2.
690 Imaging was carried out using a two-photon microscope (Scientifica) equipped with a
691 mode-locked titanium-sapphire laser (Chameleon, Coherent) tuned to 915 nm and an
692 Olympus XLUMPlanFI 20x water immersion objective (NA 0.95). To prevent eye
693 movements, the ocular muscles were paralyzed by injection of 1 nL of α-bungarotoxin
694 (2 mg/mL) behind the eye. Most imaging was carried out in the dorsal the retina.
695 The signal-to-noise ratio of the microscope was optimized by collecting photons
696 through both the objective and a sub-stage oil condenser (Olympus, NA 1.4). Emission was
697 filtered through GFP filters (HQ 535/50, Chroma Technology) before detection with GaAsP
698 photomultipliers (H7422P-40, Hamamatsu). The signal from each detector passed through
699 a current-to-voltage converter and then the two signals were added by a summing amplifier
700 before digitization. Scanning and image acquisition were controlled under ScanImage v.3.6

701 software[64]. In iGluSnFR recordings images were acquired at 10 Hz (128 × 100 pixels per
702 frame, 1 ms per line) while linescans were acquired at 1 kHz. In GCaMP recordings images
703 were acquired at 20 Hz (128 × 50 pixels per frame, 1 ms per line). Full-field light stimuli
704 were generated by an amber LED (l_{max} = 590 nm, Thorlabs), filtered through a 590/10 nm
705 BP filter (Thorlabs), and delivered through a light guide placed close to the eye of the fish.
706 These wavelengths will most effectively stimulate red and green cones but do not stimulate
707 UV cones which are enriched in the strike zone[65]. The microscope was synchronized to
708 visual stimulation. Relative changes in fluorescence ($\Delta F/F$) during a stimulus were
709 measured relative to the baseline before the stimulus.
710

711 **Stimulation protocols**

712 Only full-field stimuli were used in which light intensity was varied sinusoidally over time i.e
713 we only explored the signalling of temporal contrast. There was no variation in intensity
714 over space and the stimuli did not therefore contain any spatial contrast. Measurements
715 of contrast sensitivity with SyGCaMP2 were made by stimulating the fish with a series of
716 10 s stimuli (modulation at 5 Hz) around a mean intensity of 55 nW $mm^{-2.}$ Measurements
717 of contrast sensitivity with iGluSnFR used 2 s stimuli. To measure the distribution of events
718 amplitudes and the temporal precision fish were continuously stimulated for 30 s at a given
719 contrast.
720 Luminance sensitivity was assessed by stimulating the fish with a series of light steps
721 (4 x 3 s) at 9 different light intensities increasing in steps of 0.5 log unit steps ranging from
722 11 pW mm^{-2} to 110 nW mm^{-2} (equivalent to 3.3 x 10^{11} photons mm^{-2}).
723

724 **Drug injections**

725 Dopamine signalling was manipulated by injecting the antagonist of D1 receptors SCH
726 23390 at a final estimated concentration of 20 nM (Sigma). Finally, the long-lasting
727 dopamine receptor ligand [3H] 2-amino-6,7-dihydroxy 1,2,3,4-tetrahydronapthalene

728 (ADTN) (Sigma) was injected to a final estimated concentration of 200 nM. We confirmed
729 that these drugs gained access by including 1 mM Alexa 594 in the injection needle; within
730 5 mins of injection the dye could be detected within the inner plexiform layer of the retina.
731 Vehicle injection did not affect synaptic responses to varying contrast.
732
733 **Calculation of temporal jitter**
734 In order to quantify variability in the timing of glutamatergic events, we first calculated the
735 vector strength, r_q, for events composed of q quanta:

736
$$r_q = \frac{1}{N_q}\sqrt{\left(\sum_{i=1}^{N_q} cos\left(\frac{2\pi t_{q_i}}{T}\right)\right)^2 + \left(\sum_{i=1}^{N_q} sin\left(\frac{2\pi t_{q_i}}{T}\right)\right)^2} \quad (1)$$

737 where t_{qi} is the time of the ith q quantal event, T is the stimulus period, and N_q is the total
738 number of events composed of q quanta. The method for estimating t and q is summarized
739 in Supplementary Figure 4. The temporal jitter, J_q, can then be calculated as:

740
$$J_q = \frac{\sqrt{2(1 - r_q)}}{2\pi f} \quad (2)$$

741 where f is the stimulus frequency.
742
743 **Calculations based on Information Theory**
744 To quantify the amount of information about a visual stimulus that is contained within the
745 sequence of release events from an active zone we first needed to convert bipolar cell
746 outputs into a probabilistic framework from which we could evaluate the specific
747 information (I_2), a metric that quantifies how much information about one random
748 variable is conveyed by the observation a specific symbol of another random variable[40].
749 The time series of quantal events was converted into a probability distribution by dividing
750 into time bins of 20 ms, such that each bin contained either zero events or one event of
751 an integer amplitude. We then counted the number of bins containing events of
752 amplitude 1, or 2, or 3 etc. By dividing the number of bins of each type by the total

number of bins for each different stimulus, we obtained the conditional distribution of **Q** given **S**, $p(\boldsymbol{Q}|\boldsymbol{S})$, where **Q** is the random variable representing the *quanta/bin* and **S** is the random variable representing the *stimulus contrasts* presented throughout the course of the experiment. In the absence of information about the distribution of contrasts normally experienced by a larval zebrafish, a uniform distribution of contrasts was used for S. Each contrast step lasted 2 s (5 Hz) and they were presented in two different pseudo-random orders, of which one is shown in Fig. 4D. The contrast sensitivity varied between synapses and between morning and afternoon (Fig. 1E-G) so to make allowance for this the stimulus set S was adjusted for each synapse to span contrasts ±10% around $C_{1/2}$ measured within that synapse.

We computed the joint probability distribution by the chain rule for probability (given the experimentally defined uniform distribution of stimuli **S**):

$$\boldsymbol{p(S,Q) = p(Q|S)p(S)} \tag{7}$$

In order to convert this distribution into the conditional distribution of S given Q, we used the definition of the conditional distribution:

$$\boldsymbol{p(S|Q) = \frac{p(S,Q)}{p(Q)}} \tag{8}$$

From these distributions we computed two metrics: the mutual information I(**S;Q**)[66] and specific information I_2(**S;q**)[41]. Mutual information is defined traditionally as:

$$\mathbf{I}(\boldsymbol{S};\boldsymbol{Q}) = \boldsymbol{H(S) - H(S|Q)} \tag{9}$$

$$\mathbf{I}(\boldsymbol{S};\boldsymbol{Q}) = \sum_{\boldsymbol{s}\in\boldsymbol{S}}\sum_{\boldsymbol{q}\in\boldsymbol{Q}} \boldsymbol{p(s,q)}\,\mathbf{log_2}\,\boldsymbol{\frac{p(s)p(q)}{p(s,q)}} = \boldsymbol{I(Q;S)} \tag{10}$$

The specific information, I_2(**S;q**), is defined as the difference between the entropy of the stimulus S minus the conditional entropy of the stimulus given the observed symbol in the response q:

$$\boldsymbol{I_2(S,q) = H(S) - H(S|q)} \tag{11}$$

$$\boldsymbol{I_2(S,q) = -\sum_{s\in S} p(s)\,log\,p(s) + \sum_{s\in S} p(s|q)\,log\,p(s|q)} \tag{12}$$

representing the amount of information observing each quantal event type q ϵ **Q** carries about the stimulus distribution **S**. Note that mutual information can also be computed from the specific information as the dot product of the specific information vector $\boldsymbol{I_2}$ and the vector describing the probability of an event of a given quantal size $\boldsymbol{p}(\boldsymbol{q})$. This adds to the interpretability of both metrics – the specific information is the amount of information a single (specific) symbol gives about the stimulus, and the mutual information is the average amount of information about the stimulus gained from observing any symbol.

Measuring entropy and mutual information from neural responses can be a challenging problem. Estimates require sampling from an unknown discrete probability distribution, and in many cases recording sufficient samples to observe all non-zero probability events is neither tractable nor practical. The biases introduced by undersampling can be a particular problem when the full support of the distribution (all values that map to non-zero probabilities) is high. Within the past few decades, various approaches to correcting biases in information theoretic analyses have been developed[67]. However, as the distributions of interest in this work have both a small support and are well sampled, we have opted to use standard estimates for the quantities of interest.

Statistics

All data are given as mean ± s.e.m. unless otherwise stated in the figure legends. All statistical tests met appropriate assumptions and were calculated using inbuilt functions in IgorPro (Wavemetrics). When data were not normally distributed we used non-parametric tests. Significance was defined as $p < 0.05$. Data collection was not randomized because all experiments were carried out within one set of animals. Delivery of different stimuli was randomized where appropriate. Data were only excluded from the analysis if the signal-to-noise ratio (SNR) of the iGluSnFR signals elicited at a given synapse was not sufficient to detect unitary responses to visual stimuli with a SNR of at least three.

805 **Data Availability**

806 Source data are provided with this paper. The datasets generated during and/or
807 analysed during the current study are available from the corresponding author on
808 reasonable request.

809

810 **Code Availability**

811 Custom code used for data analysis is available on request to Leon Lagnado.

812

813

814 ## References

815

816 1 Bargmann, C. I. & Marder, E. From the connectome to brain function. *Nat Methods* **10**, 483-
817 490, doi:nmeth.2451 [pii] 10.1038/nmeth.2451 (2013).

818 2 Kastner, D. B. & Baccus, S. A. Coordinated dynamic encoding in the retina using opposing
819 forms of plasticity. *Nature neuroscience* **14**, 1317 (2011).

820 3 Johnston, J. *et al.* A Retinal Circuit Generating a Dynamic Predictive Code for Oriented
821 Features. *Neuron* **102**, 1211-1222 e1213, doi:10.1016/j.neuron.2019.04.002 (2019).

822 4 Esposti, F., Johnston, J., Rosa, J. M., Leung, K. M. & Lagnado, L. Olfactory stimulation
823 selectively modulates the OFF pathway in the retina of zebrafish. *Neuron* **79**, 97-110,
824 doi:10.1016/j.neuron.2013.05.001 (2013).

825 5 Schroder, S. *et al.* Arousal Modulates Retinal Output. *Neuron* **107**, 487-495 e489,
826 doi:10.1016/j.neuron.2020.04.026 (2020).

827 6 Ribelayga, C., Cao, Y. & Mangel, S. C. The circadian clock in the retina controls rod-cone
828 coupling. *Neuron* **59**, 790-801, doi:10.1016/j.neuron.2008.07.017 (2008).

829 7 Li, L. Circadian Vision in Zebrafish: From Molecule to Cell and from Neural Network to Behavior.
830 *J Biol Rhythms* **34**, 451-462, doi:10.1177/0748730419863917 (2019).

831 8 Roy, S. & Field, G. D. Dopaminergic modulation of retinal processing from starlight to sunlight.
832 *J Pharmacol Sci* **140**, 86-93, doi:10.1016/j.jphs.2019.03.006 (2019).

833 9 Zang, J. *et al.* Circadian regulation of vertebrate cone photoreceptor function. *eLife* **10**, e68903,
834 doi:10.7554/eLife.68903 (2021).

835 10 Wagner, H.-J. Light-dependent plasticity of the morphology of horizontal cell terminals in cone
836 pedicles of fish retinas. *Journal of neurocytology* **9**, 573-590 (1980).

837 11 Jackson, C. R. *et al.* Retinal dopamine mediates multiple dimensions of light-adapted vision.
838 *The Journal of neuroscience : the official journal of the Society for Neuroscience* **32**, 9359-9368,
839 doi:10.1523/JNEUROSCI.0711-12.2012 (2012).

840 12 Euler, T., Haverkamp, S., Schubert, T. & Baden, T. Retinal bipolar cells: elementary building
841 blocks of vision. *Nat Rev Neurosci* **15**, 507-519, doi:10.1038/nrn3783 (2014).

13 Nikolaev, A., Leung, K. M., Odermatt, B. & Lagnado, L. Synaptic mechanisms of adaptation and sensitization in the retina. *Nat Neurosci* **16**, 934-941, doi:10.1038/nn.3408 (2013).

14 Zimmermann, M. J. Y. *et al.* Zebrafish Differentially Process Color across Visual Space to Match Natural Scenes. *Curr Biol* **28**, 2018-2032.e2015, doi:10.1016/j.cub.2018.04.075 (2018).

15 Matsumoto, A. *et al.* Direction selectivity in retinal bipolar cell axon terminals. *Neuron* (2021).

16 Lagnado, L. & Schmitz, F. Ribbon Synapses and Visual Processing in the Retina. *Annu Rev Vis Sci* **1**, 235-262, doi:10.1146/annurev-vision-082114-035709 (2015).

17 Glowatzki, E. & Fuchs, P. A. Transmitter release at the hair cell ribbon synapse. *Nat Neurosci* **5**, 147-154, doi:10.1038/nn796 (2002).

18 Singer, J. H., Lassova, L., Vardi, N. & Diamond, J. S. Coordinated multivesicular release at a mammalian ribbon synapse. *Nat Neurosci* **7**, 826-833, doi:10.1038/nn1280 (2004).

19 James, B., Darnet, L., Moya-Diaz, J., Seibel, S. H. & Lagnado, L. An amplitude code transmits information at a visual synapse. *Nat Neurosci* **22**, 1140-1147, doi:10.1038/s41593-019-0403-6 (2019).

20 Lisman, J. E., Raghavachari, S. & Tsien, R. W. The sequence of events that underlie quantal transmission at central glutamatergic synapses. *Nat Rev Neurosci* **8**, 597-609, doi:10.1038/nrn2191 (2007).

21 Huang, C.-H., Bao, J. & Sakaba, T. Multivesicular Release Differentiates the Reliability of Synaptic Transmission between the Visual Cortex and the Somatosensory Cortex. *The Journal of Neuroscience* **30**, 11994, doi:10.1523/JNEUROSCI.2381-10.2010 (2010).

22 Holler, S., Köstinger, G., Martin, K. A. C., Schuhknecht, G. F. P. & Stratford, K. J. Structure and function of a neocortical synapse. *Nature* **591**, 111-116, doi:10.1038/s41586-020-03134-2 (2021).

23 Shannon, C. A Mathematical Theory of Communication. *Bell System Technical Journal* **27**, 379-423 (1948).

24 Borst, A. & Theunissen, F. E. Information theory and neural coding. *Nat Neurosci* **2**, 947-957, doi:10.1038/14731 (1999).

25 Marvin, J. S. *et al.* An optimized fluorescent probe for visualizing glutamate neurotransmission. *Nat Methods* **10**, 162-170, doi:10.1038/nmeth.2333 (2013).

26 Dreosti, E., Odermatt, B., Dorostkar, M. M. & Lagnado, L. A genetically encoded reporter of synaptic activity in vivo. *Nat Methods* **6**, 883-889, doi:10.1038/nmeth.1399 (2009).

27 Emran, F., Rihel, J., Adolph, A. R. & Dowling, J. E. Zebrafish larvae lose vision at night. *Proceedings of the National Academy of Sciences* **107**, 6034, doi:10.1073/pnas.0914718107 (2010).

28 Nie, K. *et al.* Effects of circadian clock protein Per1b on zebrafish visual functions. *Chronobiology international* **35**, 160-168 (2018).

29 Ashmore, J. & Copenhagen, D. An analysis of transmission from cones to hyperpolarizing bipolar cells in the retina of the turtle. *The Journal of Physiology* **340**, 569-597 (1983).

30 Dayan, P. & Abbott, L. F. *Theoretical neuroscience: computational and mathematical modeling of neural systems*. (MIT press, 2005).

31 Smith, R. G. & Dhingra, N. K. Ideal observer analysis of signal quality in retinal circuits. *Progress in Retinal and Eye Research* **28**, 263-288, doi:https://doi.org/10.1016/j.preteyeres.2009.05.001 (2009).

32 Faisal, A. A., Selen, L. P. & Wolpert, D. M. Noise in the nervous system. *Nat Rev Neurosci* **9**, 292-303, doi:10.1038/nrn2258 (2008).

885 33 Rusakov, D. A., Savtchenko, L. P. & Latham, P. E. Noisy Synaptic Conductance: Bug or a
886 Feature? *Trends Neurosci* **43**, 363-372, doi:10.1016/j.tins.2020.03.009 (2020).

887 34 Berry, M. J., Warland, D. K. & Meister, M. The structure and precision of retinal spike trains.
888 *Proceedings of the National Academy of Sciences* **94**, 5411, doi:10.1073/pnas.94.10.5411 (1997).

889 35 Churchland, M. M. *et al.* Stimulus onset quenches neural variability: a widespread cortical
890 phenomenon. *Nature Neuroscience* **13**, 369-378, doi:10.1038/nn.2501 (2010).

891 36 Rathbun, D. L., Warland, D. K. & Usrey, W. M. Spike timing and information transmission at
892 retinogeniculate synapses. *Journal of Neuroscience* **30**, 13558-13566 (2010).

893 37 Cui, Y., Wang, Y. V., Park, S. J. H., Demb, J. B. & Butts, D. A. Divisive suppression explains
894 high-precision firing and contrast adaptation in retinal ganglion cells. *eLife* **5**, e19460,
895 doi:10.7554/eLife.19460 (2016).

896 38 Freed, M. A. Quantal encoding of information in a retinal ganglion cell. *J Neurophysiol* **94**, 1048-
897 1056, doi:10.1152/jn.01276.2004 (2005).

898 39 Odermatt, B., Nikolaev, A. & Lagnado, L. Encoding of luminance and contrast by linear and
899 nonlinear synapses in the retina. *Neuron* **73**, 758-773, doi:10.1016/j.neuron.2011.12.023 (2012).

900 40 Stone, J. V. *Principles of Neural Information Theory: Computational Neuroscience and*
901 *Metabolic Efficiency* (Sebtel Press, 2018).

902 41 DeWeese, M. R. & Meister, M. How to measure the information gained from one symbol.
903 *Network* **10**, 325-340 (1999).

904 42 Attwell, D. & Laughlin, S. B. An energy budget for signaling in the grey matter of the brain.
905 *Journal of Cerebral Blood Flow & Metabolism* **21**, 1133-1145 (2001).

906 43 Harris, Julia J., Jolivet, R. & Attwell, D. Synaptic Energy Use and Supply. *Neuron* **75**, 762-777,
907 doi:https://doi.org/10.1016/j.neuron.2012.08.019 (2012).

908 44 Koch, K. *et al.* How much the eye tells the brain. *Curr Biol* **16**, 1428-1434,
909 doi:10.1016/j.cub.2006.05.056 (2006).

910 45 Storch, K. F. *et al.* Intrinsic circadian clock of the mammalian retina: importance for retinal
911 processing of visual information. *Cell* **130**, 730-741, doi:10.1016/j.cell.2007.06.045 (2007).

912 46 Besharse, J. C. & McMahon, D. G. The Retina and Other Light-sensitive Ocular Clocks. *Journal*
913 *of biological rhythms* **31**, 223-243, doi:10.1177/0748730416642657 (2016).

914 47 Goel, M. & Mangel, S. C. Dopamine-Mediated Circadian and Light/Dark-Adaptive Modulation
915 of Chemical and Electrical Synapses in the Outer Retina. *Front Cell Neurosci* **15**, 647541,
916 doi:10.3389/fncel.2021.647541 (2021).

917 48 Mora-Ferrer, C., Yazulla, S., Studholme, K. M. & Haak-Frendscho, M. Dopamine D1-receptor
918 immunolocalization in goldfish retina. *Journal of Comparative Neurology* **411**, 705-714 (1999).

919 49 Farshi, P., Fyk-Kolodziej, B., Krolewski, D. M., Walker, P. D. & Ichinose, T. Dopamine D1
920 receptor expression is bipolar cell type-specific in the mouse retina. *The Journal of comparative*
921 *neurology* **524**, 2059-2079, doi:10.1002/cne.23932 (2016).

922 50 Li, P. *et al.* Cloning and spatial and temporal expression of the zebrafish dopamine D1 receptor.
923 *Dev Dyn* **236**, 1339-1346, doi:10.1002/dvdy.21130 (2007).

924 51 Hull, C., Studholme, K., Yazulla, S. & von Gersdorff, H. Diurnal changes in exocytosis and the
925 number of synaptic ribbons at active zones of an ON-type bipolar cell terminal. *J Neurophysiol* **96**,
926 2025-2033, doi:10.1152/jn.00364.2006 (2006).

927 52 Mazade, R. E., Flood, M. D. & Eggers, E. D. Dopamine D1 receptor activation reduces local
928 inner retinal inhibition to light-adapted levels. *J Neurophysiol* **121**, 1232-1243,
929 doi:10.1152/jn.00448.2018 (2019).

930 53 Travis, A. M., Heflin, S. J., Hirano, A. A., Brecha, N. C. & Arshavsky, V. Y. Dopamine-dependent
931 sensitization of rod bipolar cells by GABA is conveyed through wide-field amacrine cells. *Journal of*
932 *Neuroscience* **38**, 723-732 (2018).

933 54 Ribelayga, C., Wang, Y. & Mangel, S. C. A circadian clock in the fish retina regulates dopamine
934 release via activation of melatonin receptors. *The Journal of Physiology* **554**, 467-482,
935 doi:https://doi.org/10.1113/jphysiol.2003.053710 (2004).

936 55 Moya-Díaz, J., James, B. & Lagnado, L. Modulation of the vesicle code transmitting the visual
937 signal in the retina. *bioRxiv*, 2020.2004.2022.056119, doi:10.1101/2020.04.22.056119 (2020).

938 56 Thermos, K. Functional mapping of somatostatin receptors in the retina: a review. *Vision*
939 *Research* **43**, 1805-1815, doi:https://doi.org/10.1016/S0042-6989(03)00169-X (2003).

940 57 Freed, M. A. & Liang, Z. Synaptic noise is an information bottleneck in the inner retina during
941 dynamic visual stimulation. *The Journal of physiology* **592**, 635-651,
942 doi:10.1113/jphysiol.2013.265744 (2014).

943 58 McDonnell, M. D. & Ward, L. M. The benefits of noise in neural systems: bridging theory and
944 experiment. *Nature Reviews Neuroscience* **12**, 415-425, doi:10.1038/nrn3061 (2011).

945 59 Vigh, J., Vickers, E. & von Gersdorff, H. Light-evoked lateral GABAergic inhibition at single
946 bipolar cell synaptic terminals is driven by distinct retinal microcircuits. *Journal of Neuroscience* **31**,
947 15884-15893 (2011).

948 60 Christie, J. M. & Jahr, C. E. Multivesicular release at Schaffer collateral-CA1 hippocampal
949 synapses. *The Journal of neuroscience : the official journal of the Society for Neuroscience* **26**, 210-
950 216, doi:10.1523/JNEUROSCI.4307-05.2006 (2006).

951 61 Auger, C., Kondo, S. & Marty, A. Multivesicular release at single functional synaptic sites in
952 cerebellar stellate and basket cells. *The Journal of neuroscience : the official journal of the Society*
953 *for Neuroscience* **18**, 4532-4547 (1998).

954 62 Higley, M. J., Soler-Llavina, G. J. & Sabatini, B. L. Cholinergic modulation of multivesicular
955 release regulates striatal synaptic potency and integration. *Nature neuroscience* **12**, 1121-1128
956 (2009).

957 63 Chalifoux, J. R. & Carter, A. G. GABAB receptors modulate NMDA receptor calcium signals in
958 dendritic spines. *Neuron* **66**, 101-113 (2010).

959 64 Pologruto, T. A., Sabatini, B. L. & Svoboda, K. ScanImage: flexible software for operating laser
960 scanning microscopes. *Biomed Eng Online* **2**, 13, doi:10.1186/1475-925X-2-13 (2003).

961 65 Yoshimatsu, T., Schröder, C., Nevala, N. E., Berens, P. & Baden, T. Fovea-like Photoreceptor
962 Specializations Underlie Single UV Cone Driven Prey-Capture Behavior in Zebrafish. *Neuron* **107**,
963 320-337.e326, doi:10.1016/j.neuron.2020.04.021 (2020).

964 66 de Ruyter van Steveninck, R. R., Lewen, G. D., Strong, S. P., Koberle, R. & Bialek, W.
965 Reproducibility and variability in neural spike trains. *Science* **275**, 1805-1808,
966 doi:10.1126/science.275.5307.1805 (1997).

967 67 Pola, G., Schultz, S. R, Petersen, R. S & Panzeri, S. in *Neuroscience Databases: A Practical*
968 *Guide* (Springer, Boston, MA, 2003).

969

970

Acknowledgements

The authors express many thanks to all the members of Lagnado laboratory for discussion. We also thank Tom Baden and Sylvia Schröder for their criticisms and suggestions. This work was supported by grants to L.L. from the Wellcome Trust (102905/Z/13/Z and 221936/Z/20/Z).

Author contributions

J. M-D. conceived, designed and executed experiments, analyzed results and prepared the manuscript. B. J. carried out analysis and wrote code. F. E. conceived and executed experiments and carried out analysis. J. J. conceived and executed experiments and carried out analysis. L. L. conceived the project, designed experiments, analyzed data, repaired equipment, wrote code and prepared the manuscript.

Competing Interests

The authors declare that they have no competing interests.

Diurnal changes in the efficiency of information transmission at a sensory synapse

José Moya-Díaz, Ben James, Federico Esposti, Jamie Johnston and Leon Lagnado*

Supplementary Information (Figures S1-S4)

Supplementary Figure 1

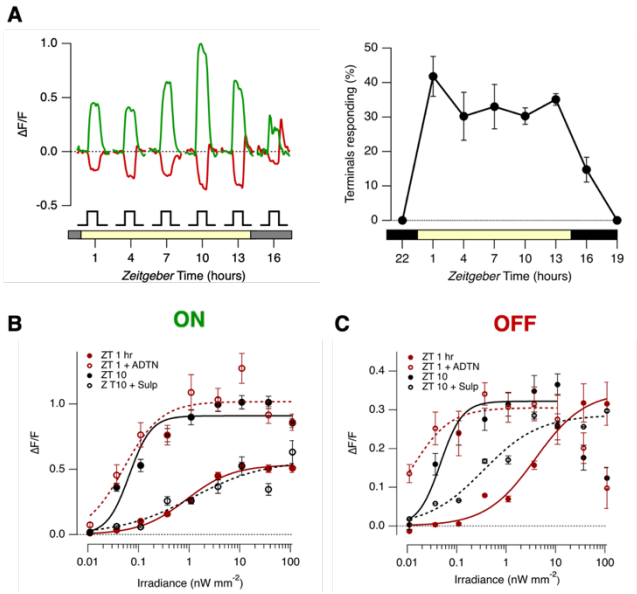

Figure S1. Diurnal changes in luminance sensitivity are co-ordinated by dopamine

A. Left: Averaged SyGCaMP2 signals at different *Zeitgeber* time. ON terminals green (n = 535 from 38 fish) and OFF terminals red (n = 355 from 38 fish). Each step of light (10 nW mm^{-2}) lasted 3 s. These averages are only from responsive terminals. Right: the percentage of terminals generating a significant response to the same light step (averaged across both ON and OFF). Bars show SD. **B.** Effects of manipulating dopamine signalling on luminance sensitivity of the ON channel. Luminance vs. response plots for ON terminals. Red circles compare this function at ZT 1 hr under control conditions (solid circle) and after injection of the dopamine receptor agonist ADTN (~0.2 μM; open circles). ADTN caused a prompt change in the luminance-response function to forms measured at ZT 10 hrs (solid black circles), increasing R_{max} from 0.53 ± 0.02 to 1.02 ± 0.07, and reducing $I_{1/2}$ from 0.88 ± 0.18 nW mm^{-2} to 0.05 ± 0.02 nW mm^{-2} (± sd, as estimated from the fitted Hill function shown). The higher gain and luminance sensitivity at ZT 10 hrs could be explained as an effect of dopamine at D2 receptors, because it was completely reversed by injection of the selective D2 receptor antagonist sulpiride (~2 μM; open black circles; R_{max} = 0.57 ± 0.13, $I_{1/2}$ = 1.16 ± 1.34 nW mm^{-2}). Results collected from *n* = 535 terminals from 38 fish. **C.** Effects of manipulating dopamine signalling on luminance sensitivity of the OFF channel. Comparing control responses at ZT 1 hr and 10 hrs showed a significant reduction in $I_{1/2}$ from 3.9 ± 1.3 to 0.0128 ± 0.005, but *without* a significant change in R_{max} (0.35 ± 0.03 vs 0.30 ± 0.02). ADTN injected at ZT 1 caused a prompt increase in luminance sensitivity, reducing $I_{1/2}$ to 0.013 ± 0.005 nW mm^{-2}. The higher luminance sensitivity at ZT 10 hrs could be partly explained as an effect of dopamine at D2 receptors, because injection of sulpiride (~2 μM; open black circles) increased $I_{1/2}$ from 0.05 ± 0.01 nW mm^{-2} to 0.35 ± 0.14 nW mm^{-2}. Results collected from *n* = 355 terminals from 38 fish.

Supplementary Figure 2

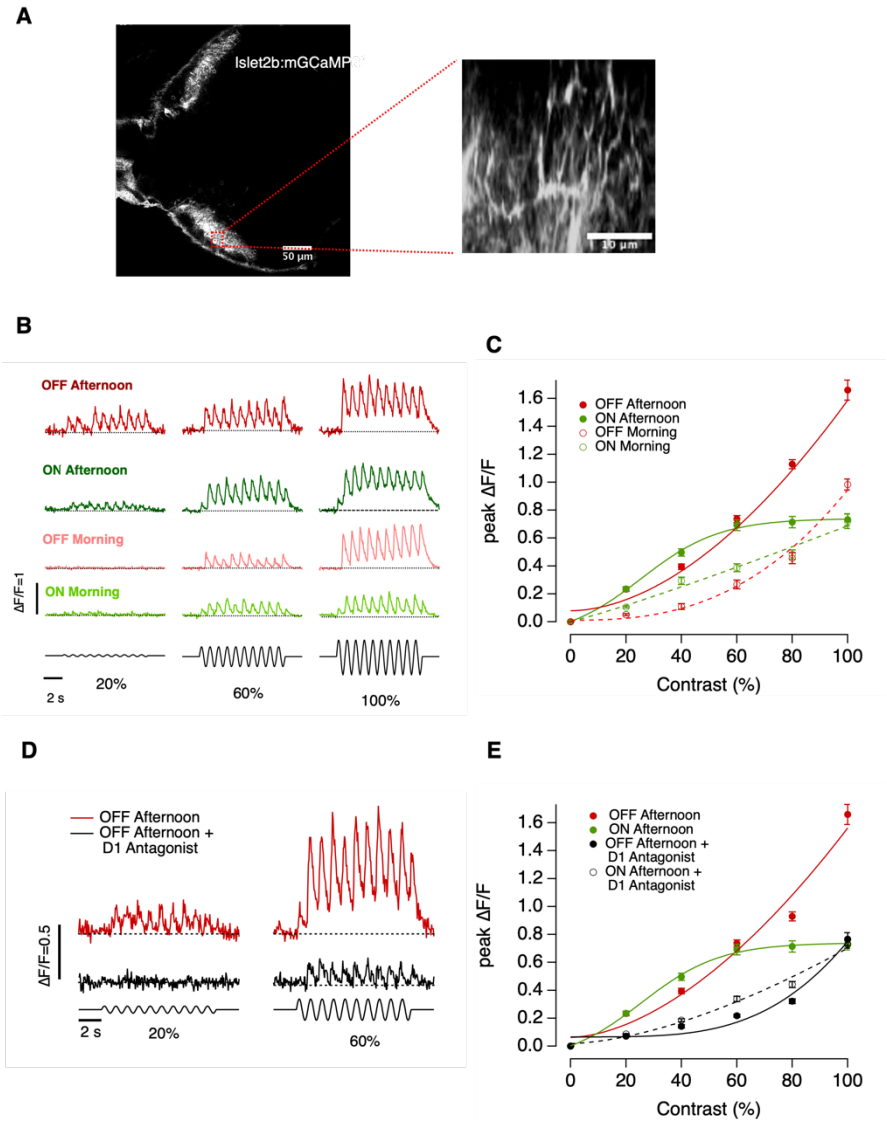

Figure S2. Diurnal changes in the visual signal delivered to the optic tectum

A.*Left panel*. Multiphoton section through the tectum of a zebrafish larva islet2b:mGCaMP6f (7 dpf) expressing the calcium reporter mGCaMP6f, which labels axons and synaptic terminals of retinal ganglion cells (RGCs). *Right panel*. Blow-up of the square red shown in the left panel. The image shows the Z plane reconstruction from where the synaptic responses were recorded. **B.** mGCaMP6f signals from individual ON and OFF RGCs synapses elicited using a stimulus contrast of 20%,60% and 100 %. Note that here the stimulus was modulated at 1 Hz (full field, sine wave) rather than the 5 Hz used in the main body of the paper. **C.** Average contrast-response functions displayed by ON and OFF RGCs, where the response (*R*) was quantified as the average of the fluorescence peak amplitudes measured at each cycle of stimulation. Note the differences in the magnitude of the responses between OFF RGCs in the morning relative to afternoon. Each point shows the mean ± s.e.m. Number of RGCs is: ON afternoon, 14; OFF afternoon, 13; ON morning, 11; OFF morning, 12. **D.** mGCaMP6f signals from an individual OFF RGCs before and after intravitreal injection of the D1 antagonist in the afternoon. **E.** Average contrast-response function displayed by ON and OFF RGCs before and after administration of the D1 antagonist in the afternoon. Note the dramatic decrease in the magnitude of the response in both ON and OFF channels.

1052 **Supplementary Figure 3**

1053

1054 1055 1056 1057 1058 1059 1060

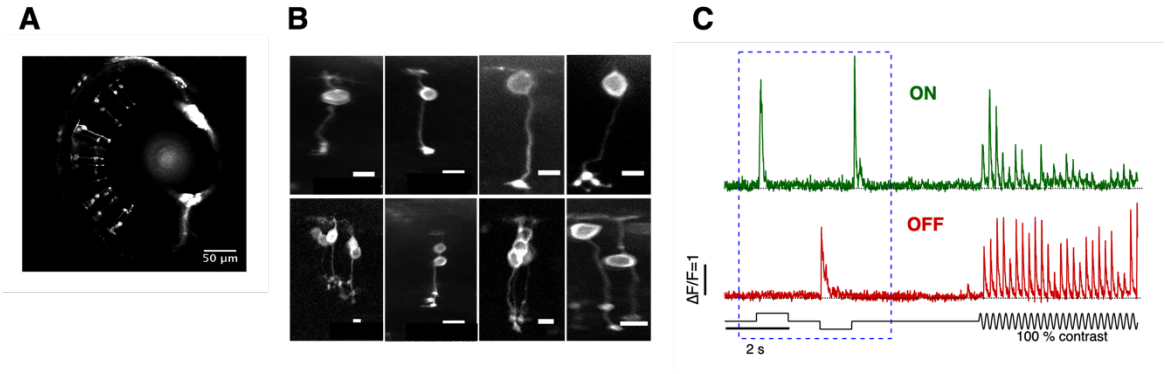

1061

1062 **Figure S3. Examples of the different morphological types of bipolar cell sampled in this study.**
1063 **A.** Multiphoton section through the eye of a larval zebrafish (7 dpf) expressing iGluSnFr in a subset of bipolar cells. **B.**
1064 Examples of some of the different morphological subtypes of OFF (top) and ON (bottom) bipolar cell which were
1065 sampled in this study. All scale bars are 2 µm. **C.** We focused on a comparison on the two most basic functional types,
1066 ON and OFF cells, identified through their responses to steps of light applied before applying stimuli modulated at 5
1067 Hz. iGluSnFR signals were measured in a total of 91 synapses in ON and 151 synapses in OFF cells.

1068
1069
1070
1071

Supplementary Figure 4

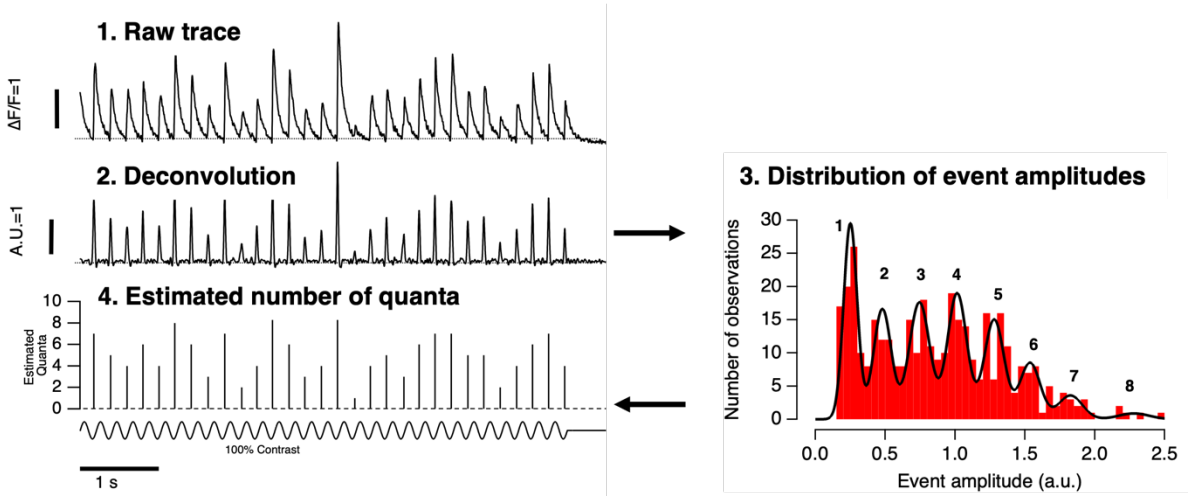

Figure S4. Decomposition of iGluSnFR signals into vesicle counts

Summary of the basic steps for quantal decomposition of iGluSnFr signals. Each event is assigned a time, t, and an estimated number of quanta, q, using the following basic steps.

1. Raw trace extracted from individual active zones (linescan, 1 KHz).

2. Trace deconvolved using the estimated Wiener filter and threshold crossings used to detect events above noise. The timing of the peak is the event time t. The amplitude of the event is the peak of the deconvolved trace at time t.

3. The distribution of event amplitudes is plotted and fitted by the sum of Gaussians with peaks differing by integer multiples of a quantal value q. This example is a histogram of event amplitudes for an active zone in which 373 events were accumulated using stimulus contrasts of 20%, 60% and 100% and a frequency of 5 Hz. The black line is a fit of eight Gaussians, identified using a Gaussian mixture model. Note that the variance of successive Gaussians did not increase in proportion to the peak number. The first peak had a value of 0.24, and the distance between peaks averaged 0.25, indicating the existence of a quantal event equivalent to ~0.25.

4. Maximum-likelihood estimation of the number of quanta, q, in each event based on its amplitude in 2 and the distribution in 3.

These steps are explained and validated in much greater detail in James et al. (2019).